PHILOSOPHICAL TRANSACTIONS OF THE ROYAL SOCIETY B BIOLOGICAL SCIENCES

Ultrastructural Studies of Spermatogenesis in Antalis entalis (Scaphopoda, Mollusca)

S. T. Hou and W. L. Maxwell

Phil. Trans. R. Soc. Lond. B 1991 **333**, 101-110
doi: 10.1098/rstb.1991.0062

Ultrastructural studies of spermatogenesis in *Antalis entalis* (Scaphopoda, Mollusca)

S. T. HOU AND W. L. MAXWELL

Department of Anatomy, University of Glasgow, Glasgow G12 8QQ, U.K.

CONTENTS

SUMMARY

Mature spermatozoa and spermatogenesis of *Antalis entalis* were studied by light, scanning and transmission electron microscopy. During spermatogenesis the spherical proacrosome arises from a single Golgi complex, migrates toward the anterior pole of the spermatid, and there differentiates to form an electron-dense collar. This is unique among examples of the simple acrosome of primitive spermatozoa. Nuclear condensation does not occur until the proacrosome and mitochondria migrate towards the future anterior and posterior poles of the spermatid. Chromatin condensation occurs by the formation of heterochromatin granules. No manchette of microtubules is observed in the course of nuclear condensation and elongation. Mitochondria achieve their mature spherical shape by decreasing in number and increasing in diameter at an early stage of spermiogenesis. No inter-mitochondrial or mitochondria-nuclear (or centriolar) junctions occur. The centriolar satellite is formed in association with the distal centriole late in spermiogenesis. Earlier, the typical '9+2' microtubular axoneme is coiled within the spermatid cytoplasm and the flagellum emerges only late in spermiogenesis. Beta glycogen granules appear late in the development of the spermatid, and are distributed in the centriolar and periacrosomal regions.

1. INTRODUCTION

Spermatogenesis and spermiogenesis in most of the molluscan classes have been studied: for example, Aplacophora (Buckland-Nicks & Chia 1989), Polyplacophora (Russell-Pinto *et al.* 1984; Sakker 1984; Buckland-Nicks *et al.* 1988; Hodgson *et al.* 1988), Bivalvia (see review, Popham 1979), Gastropoda (see review in Maxwell 1983; Healy 1988) and Cephalopoda (Maxwell 1974, 1975). Preliminary light microscopical observations of sperm and spermiogenesis in *Dentalium entalis* (= *Antalis entalis* Linné 1758, C. P. Palmer, personal communication) were provided by Retzius (1905) and Franzén (1955). Franzén (1955) classified the form of the scaphopod spermatozoon as belonging to the so-called 'primitive' group. A description of the fine structure of the mature spermatozoon confirming the primitive form of the spermatozoon of *Dentalium vulgare* and morphological changes occurring during fertilization has been provided by Dufresne-Dube *et al.* (1983). However, ultrastructural information concerning spermatogenesis and spermiogenesis of Scaphopoda is lacking.

In this paper we describe the ultrastructural changes during spermatogenesis of *Antalis entalis*, and compare its structure with that of *Dentalium vulgare* and other molluscan groups possessing the 'primitive' type of spermatozoon.

2. MATERIAL AND METHODS

Antalis entalis (Linné 1785) were collected from the University Marine Biological Station, Millport, Scotland, between March and June 1989. Animals with a shell of length greater than 39 mm, with a mature, white testis, were selected for study.

(*a*) *Light microscopy*

Animals were dissected under a stereomicroscope and small portions of testis were transferred to Bouin's fluid or Karnovsky's fixative. After 6 h of fixation at room temperature, portions of testis were dehydrated through ascending concentrations of ethanol and embedded in paraffin wax. Sections (5 μm) were cut, stained with haematoxylin and eosin (H&E) and examined with a Leitz Vario-Orthomat microscope.

(*b*) *Transmission electron microscopy* (TEM)

Small portions of testis were fixed, either for 1.5 h in 2.5% glutaraldehyde in 0.1 M sodium cacodylate buffer and seawater, or in 2.5% glutaraldehyde in seawater (1182 mOsm†) (Hodgson & Bernard 1988). After fixation for 1 h and rinsing in the corresponding buffer, the testis was postfixed in 1% osmium tetroxide in 0.1 M sodium cacodylate and seawater, dehydrated through ascending concentrations of ethanol, propylene oxide and embedded in Araldite resin. Semithin (1 μm thick) and thin sections were cut on a Reichert–Jung Ultracut. Thin sections (gold and silver colours) were collected either on copper grids, stained with uranyl acetate and lead citrate, or on nickel grids and stained with periodic acid-thiosemicarbazide-silver proteinate (PA-TSC-SP) to demonstrate glycogen (Thiéry 1967; Vye & Fischman 1971). Control sections were first oxidized with PA, followed by 1% α-diastase digestion, than further exposed to TSC and SP. All thin sections were examined in a JEOL-100S transmission electron microscope.

(*c*) *Scanning electron microscopy* (SEM)

The testis was diced, fixed with freshly prepared 2.5% glutaraldehyde in 0.1 M sodium cacodylate buffer and seawater (pH 7.4, 1010 mOsm) and smeared onto a clean glass slide. This was air-dried, post-fixed in 1% osmium tetroxide, dehydrated with acetone, sputter coated with gold–palladium and examined in a JEOL-300T scanning electron microscope.

3. RESULTS

(*a*) *Testis*

Antalis entalis is dioecious, with a lobular testis located in the dorsal part of the visceral mass that almost reaches the pavilion dorsally. The testis consists of many elongated follicles which lie parallel to the long axis of the body. Each testicular follicle is limited by a basement membrane (figure 1 inset). Spermatogonia, spermatocytes, spermatids and spermatozoa occur in small groups within the lumen of the testis (figure 1).

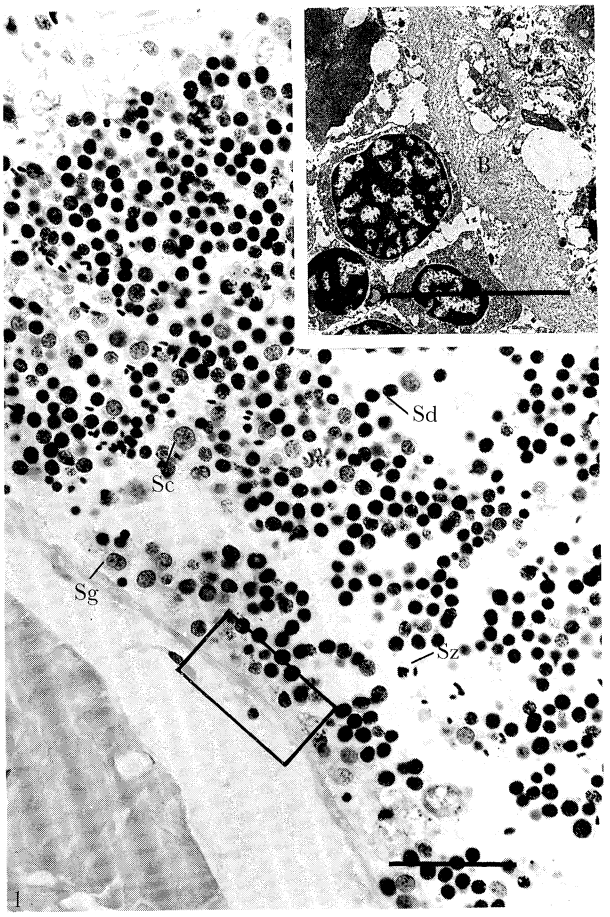

Figure 1. Light micrograph through part of the testis, showing part of a testicular follicle and developing germ cells (spermatogonium, Sg; spermatocyte, Sc; spermatid, Sd and spermatozoon, Sz). The rectangular area is enlarged to show the fibrillar basement membrane (B, inset; scale bar = 10 μm). Scale bar = 50 μm.

(*b*) *Early spermatogenesis*

The spermatogonium is a large spherical cell, closely related to the complex basement membrane limiting the testis. Its nearly spherical nucleus measures 8 ± 0.15 μm in diameter and the most prominent feature throughout this stage is the nucleolus (figure 2) (0.7 ± 0.06 μm in diameter), associated with relatively large heterochromatin aggregates within the nucleoplasm. The nucleus is surrounded by abundant cytoplasm, containing many mitochondria and a single Golgi complex. The mitochondria are uniformly distributed and about 0.4 ± 0.02 μm in diameter.

The spermatocyte has a similar size to the spermatogonium (figure 3). The absence of synaptonemal complexes indicates this is a secondary spermatocyte. The nucleus is 6 ± 0.41 μm in diameter with uniformly distributed heterochromatin through the nucleoplasm. The nucleolus is absent. Cytoplasmic organelles are very similar to those of the spermatogonium. Mito-

† One osmole contains one mole of osmotically active particles.

PHILOSOPHICAL TRANSACTIONS OF THE ROYAL SOCIETY B BIOLOGICAL SCIENCES

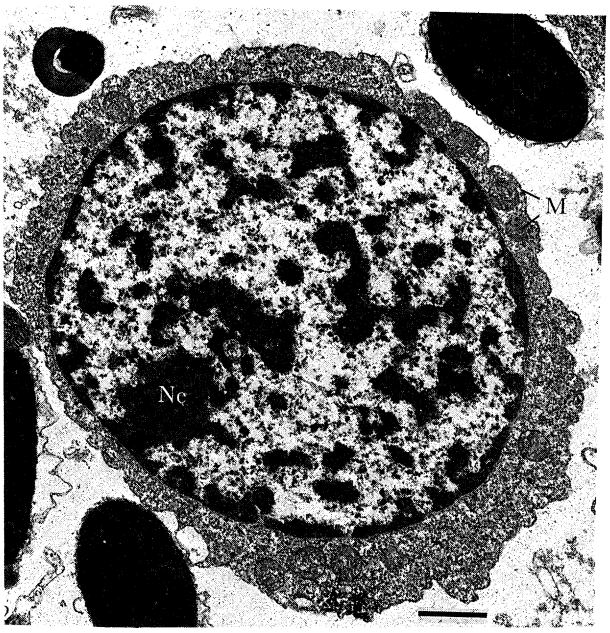

Figure 2. A spermatogonium with a prominent nucleolus (Ne), and many small mitochondria (M). Scale bar = 1 μm.

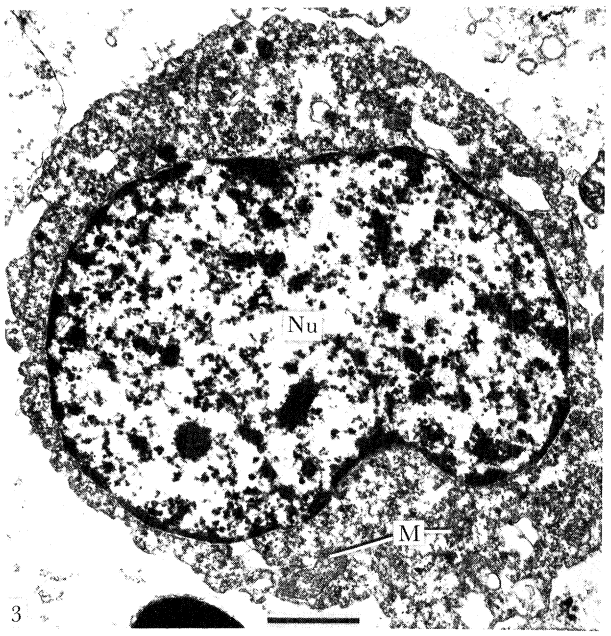

Figure 3. A secondary spermatocyte with diffuse heterochromatin in the nucleus (Nu). The mitochondria (M) are small. Scale bar = 1 μm.

chondria remain the same size as those in the spermatogonium (figure 3).

(*c*) *Spermiogenesis*

The early spermatid is of reduced size but still spherical, with a nuclear diameter of about 4 ± 0.35 μm (figure 5). Several nuclei of early spermatids often occur within a common cytoplasm (figure 4), in a manner similar to that described in bivalves, for example, *Mytilus* (Longo & Dornfeld 1967), *Neotrigonia* (Healy 1989) and *Scrobicularia plana* (Sousa *et al.* 1989). No intercellular bridges occur between spermatids.

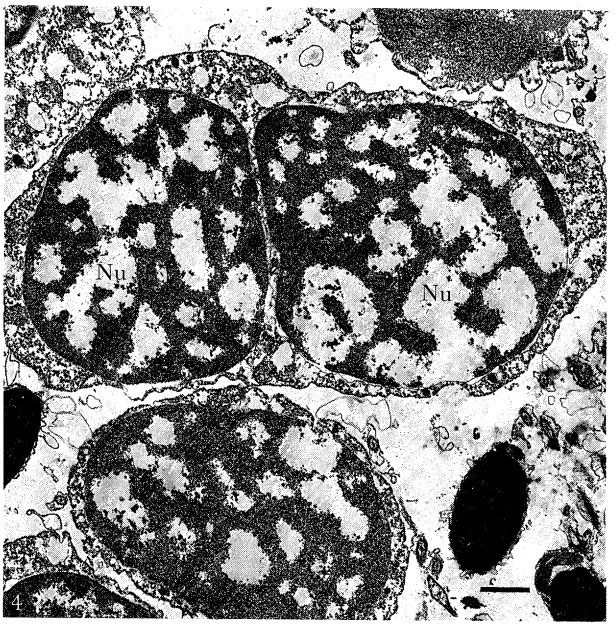

Figure 4. Two nuclei (Nu) of early spermatids occur within a single mass of cytoplasm. Scale bar = 1 μm.

Rather, there is a failure of separation of the cytoplasm derived from the spermatocyte, so that several spermatid nuclei are contained within a single cytoplasmic mass. Within the nucleus, the chromatin forms fine fibrils which then aggregate into tiny granules (about 40–95 nm in diameter, figure 5 inset). During the process of nuclear elongation in the late spermatid, these granules become closely packed (figure 6 inset), without any regular relation to the long axis of the elongating spermatid. Aggregation of the granules results in a reduction in the number of intranuclear cavities. However, a few cavities occur even in the mature spermatozoon.

When the mitochondria become apposed to the nuclear envelope (figure 7), the proacrosomal granule starts moving from the posterior towards the future anterior pole of the spermatid (figure 8). After the close apposition of the mitochondria to the posterior pole and the proacrosome to the anterior (figure 9), the longitudinal axis of the spermatid nucleus is established (we call this stage late spermatid) and in the final stage of chromatin condensation the late spermatid nucleus assumes the form of a truncated cone as the chromatin finally condenses into an almost homogeneous electron-dense state (figures 10 and 11).

Using the PA-TSC-SP technique, glycogen granules are detected at the late spermatid stage (figures 12 and 19). The granules occur in the following areas: peri-acrosomal and peri-mitochondrial. No glycogen occurs in the developing or mature tail piece.

(*d*) *Acrosome and mid-piece formation*

The pro-acrosome of *Antalis entalis* is produced by a single Golgi complex (figures 13 and 14). In the early spermatid, the Golgi complex lies close to the mitochondria and centrioles (figure 13). Two types of vesicle arise from the mature face of the Golgi body, one electron-dense, the other electron-lucent (figures

PHILOSOPHICAL TRANSACTIONS OF THE ROYAL SOCIETY B BIOLOGICAL SCIENCES

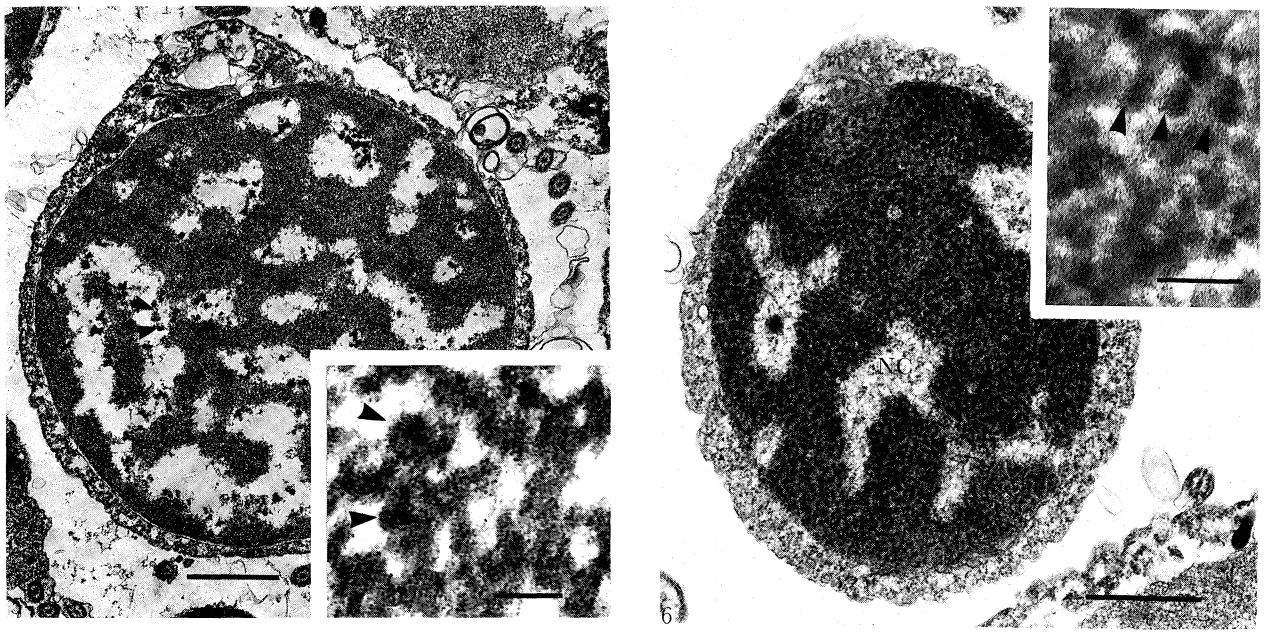

Figures 5 and 6. Sections through early (figure 5) and late (figure 6) spermatids, showing the granular heterochromatin (arrowheads in figure 5 and inset) aggregating into an almost homogeneous state (figure 6 and inset). Because of uneven chromatin condensation, small nuclear cavities (NC) remain (figure 6). Scale bars = 1 μm (0.1 μm for insets).

14 and 15). These vesicles fuse (figure 15) to form the proacrosome, a single, spherical, membrane-bound vesicle with peripheral electron-dense material surrounding a less dense centre containing granular material (figures 15 and 16). A more marked electron dense zone occurs to one side of the proacrosome (figure 16). This zone disperses to form a moderately dense layer along the inner acrosomal membrane as the proacrosome finally assumes its mature form (figure 19). Early in spermiogenesis the proacrosome underlies the plasmalemma, separated from the nucleus but closely related to the mitochondria and developing axoneme (figures 7, 8 and 16). Later, the proacrosome migrates to the surface of the nucleus so that the prominent electron-dense zone becomes apposed to the nuclear envelope (figures 9 and 17). The proacrosome then assumes the shape of an inverted cup (figure 18), with a well defined acrosomal fossa (figures 17 and 19). While the proacrosome is spherical its contents are finely granular but as the final changes in its shape occur, it becomes more electron dense (figure 17). Eventually the central electron-lucent area is lost by the apposition of the inner acrosomal membrane to the outer membrane (figures 18 and 19). The fibrous material derived from the electron dense zone mostly appears at the apex of the acrosomal fossa and close to the inner acrosomal membrane (figure 19).

At the time of proacrosome formation, mitochondria become reduced in number but increase in size; even when they become apposed to the nuclear surface they still undergo an increase in size, causing deep indentations of the base of the nucleus (figures 8, 10 and 11). The volume of each mitochondrion in the early spermatid is estimated to be about one quarter of that in the mature spermatozoon. At the early spermatid stage the centrioles lie close to the plasmalemma and lack a prominent centriolar satellite (figure 13). The developing axoneme is spirally coiled within the cytoplasm. It may lie in relation to the proacrosome or mitochondria (figures 7 and 16). The proximal centriole does not become apposed to the nuclear envelope until the late spermatid when the longitudinal axis is established. The axoneme now leaves the cell body to form the flagellum, and a centriolar satellite with nine radially arranged arms forms (figure 11 inset). Excess cytoplasm is shed to leave the truncated cone of the spermatozoan head.

(*e*) *Spermatozoon*

SEM examination of fixed spermatozoa shows the head, midpiece and tail (figures 20 and 21). The total sperm length is 116 ± 5.5 μm. The head consists of an apical acrosome and an elongated nucleus, 7.5 ± 0.6 μm long and 2.3 ± 0.1 μm wide at its base. The acrosome is a membrane-bound hollow structure surmounting the nucleus. A unique feature is the presence of a posteriorly directed invagination into the anterior region of the acrosome, forming a discrete pit (figure 20). The midpiece is of the primitive type, with five closely apposed large, spherical mitochondria (figure 21), each about 0.8 ± 0.1 μm in diameter, arranged in a circle around the centriolar complex (figure 21). The centriolar complex consists of a pair of centrioles, proximal and distal, each composed of nine typical microtubular triplets surrounded by a homogeneous electron dense matrix (figure 11 and inset). This system of centriolar satellite or anchoring fibres closely resembles the model of the centriolar satellite complex developed by Summers (1970) and Baccetti & Afzelius (1976).

PHILOSOPHICAL TRANSACTIONS OF THE ROYAL SOCIETY B BIOLOGICAL SCIENCES

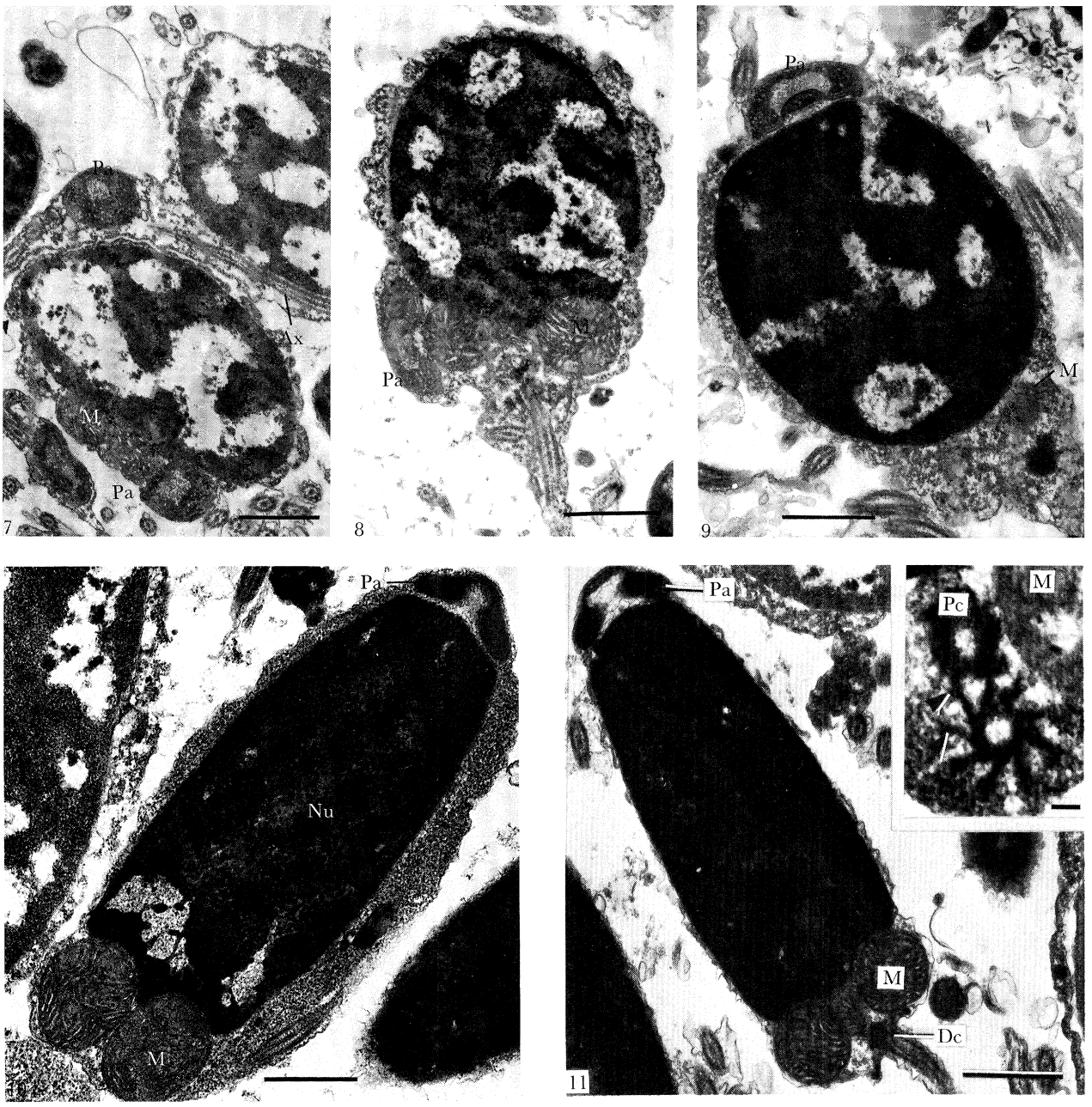

Figures 7–11. Ultrathin sections of developing early spermatids (figures 7 and 8) and late spermatids (figures 9–11). Nuclear morphogenesis results in a change from an oval shape (figure 7) to an elongate one (figures 10 and 11). The proacrosomal granule (Pa) is in close relation to mitochondria (M), axoneme (Ax) and plasmalemma in the early spermatid (figures 7 and 8) where the granular heterochromatin is still diffuse. Once the mitochondria are attached to the base of the nuclear envelope and increase in size (figure 8), the proacrosome starts to move towards the presumptive anterior pole of the spermatid. Figures 9–11 show the further condensation and elongation of the nucleus of the late spermatid and the loss of excess cytoplasm. The proximal centriole (Pc) and distal centriolar satellite (Dc) with nine radial arms (arrowheads) are fully established at this developmental stage (figure 11 inset). Scale bars = 1 μm (0.1 μm for inset).

4. DISCUSSION

Antalis entalis fertilizes externally and its spermatozoan structure falls into the so-called primitive form established by Franzén (1955). The ultrastructure of the mature spermatozoon is very similar to that of *Dentalium vulgare* (Dufresne-Dube *et al.* 1983).

The acrosome of *Antalis entalis* closely resembles that of *Dentalium vulgare* (Dufresne-Dube *et al.* 1983) and, in general, is comparable to those of Archaeogastropoda with simple acrosomes (e.g. type I spermatozoa defined by Hodgson & Bernard (1988) and some of the subtype 1A described by Koike (1985)) and those acrosomes of the Bivalvia possessing no axial rod, for example in the Veneroida and Myoida (Popham 1979). But there are several distinct structural differences. The acrosome does not form a hollow cone, but rather a ring with a centrally orientated ridge. A unique anterior

invagination or pit into the central lumen of the acrosome is formed by the external acrosomal membrane and plasmalemma. There is no variation in the electron density of the acrosomal material of the mature spermatozoon, such as occurs in types II and III spermatozoa of the patellid limpet (Hodgson & Bernard 1988) and other types of spermatozoa in archaeogastropods (Koike 1985) and bivalves (Popham 1979). Neither is an axial body or rod present in the subacrosomal space, as, for example, occurs in a wide variety of taxa (Baccetti & Afzelius 1976), e.g. *Crassostrea* (Galtsoff & Philpott 1960), *Mytilus* (Niijima & Dan 1965; Longo & Dornfeld 1976; Hodgson & Bernard 1986), *Spisula* (Longo & Anderson 1969), *Bankia* (Popham *et al.* 1974), *Donax* (Hodgson *et al.* 1990) and *Dreissena* (Franzén 1983; Maxwell 1983). In fertilization in *D. vulgare* (Dufresne-Dube *et al.* 1983), the sperm plasma membrane first fuses with the outer acrosomal membrane at this region, the acrosomal contents are then expelled through this apical pit when constriction of the outer acrosomal membrane occurs.

However, the acrosome of *A. entalis* is more complex than that of some of the primitive bivalves, for example, *Neotrigonia* (Healy 1989), in which several discoid acrosomal vesicles occur. Hinsch & Clark (1973) suggest that these simple vesicular acrosomes are the evolutionary forerunners of the acrosomal vehicle. In *Chaetoderma* sp. (Aplacophora), the vesicular acrosome,

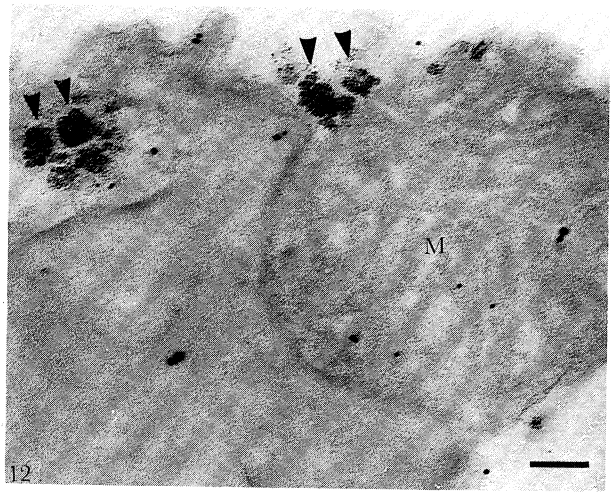

Figure 12. PA-TSC-SP treated late spermatid. Dark glycogen granules (arrowheads) occur around mitochondria (M). Scale bar = 0.1 μm.

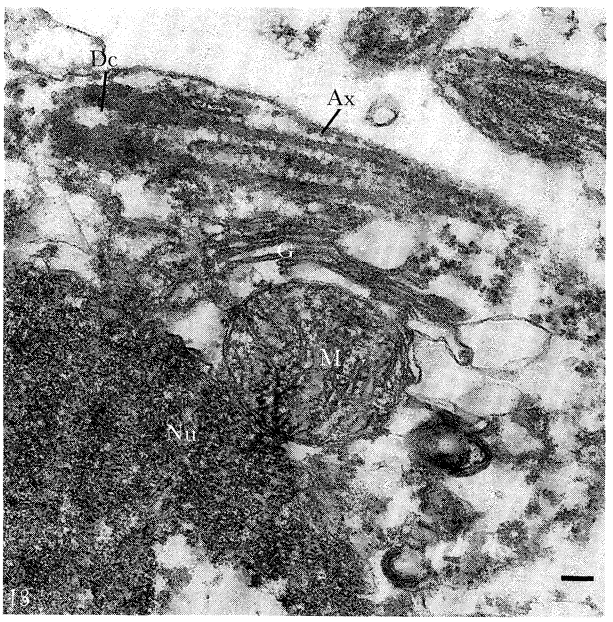

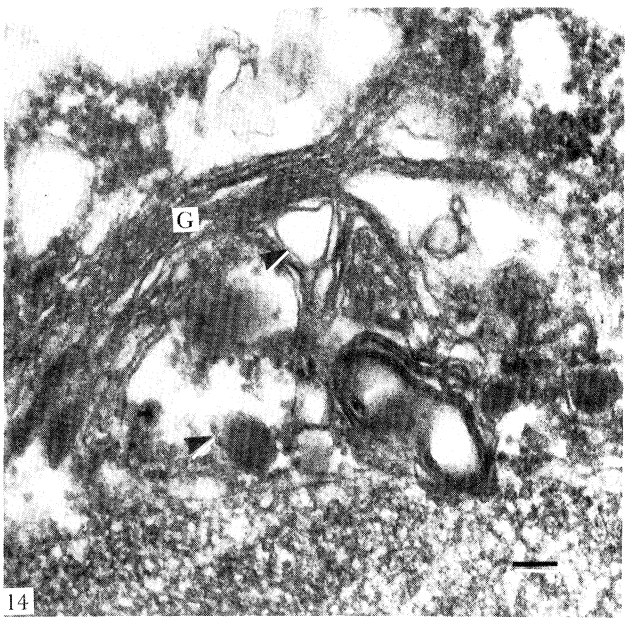

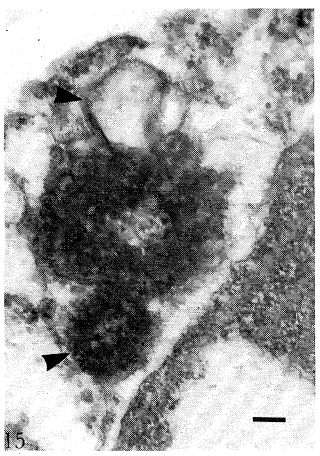

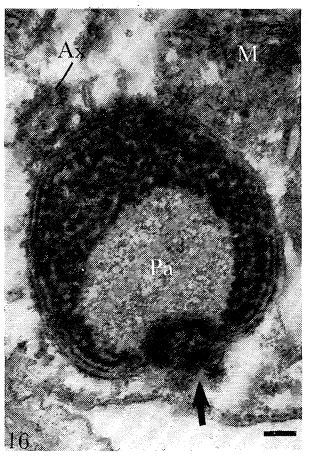

Figures 13–17. For description see opposite.

PHILOSOPHICAL TRANSACTIONS OF THE ROYAL SOCIETY B BIOLOGICAL SCIENCES

Figures 13–19. Stages of acrosome development from early spermatid (figures 13–16) to late spermatid (figures 17–19). In the early spermatid, the Golgi complex (G), mitochondria (M) and axoneme (Ax) are closely associated (figure 13). The distal centriole (Dc) at this stage lacks a supporting satellite body. Electron dense granules and lucent vesicles (arrowheads) fuse to form a proacrosomal granule (Pa) (figures 14–16). During the course of migration from the posterior to anterior pole of the spermatid, the electron-dense zone (arrows in figures 16 and 17) becomes closely related to the nucleus and gradually disperse into a layer of dense fibrous material (arrows in figure 19). The proacrosome undergoes significant morphogenesis, converting a spherical (figure 16) to a cup-shape with an inverted central pit (arrowhead) into the underlying acrosomal fossa (Af) (figures 17 and 19). Note a glycogen granule (g) close to the acrosome. Scale bar = 0.1 μm for all parts.

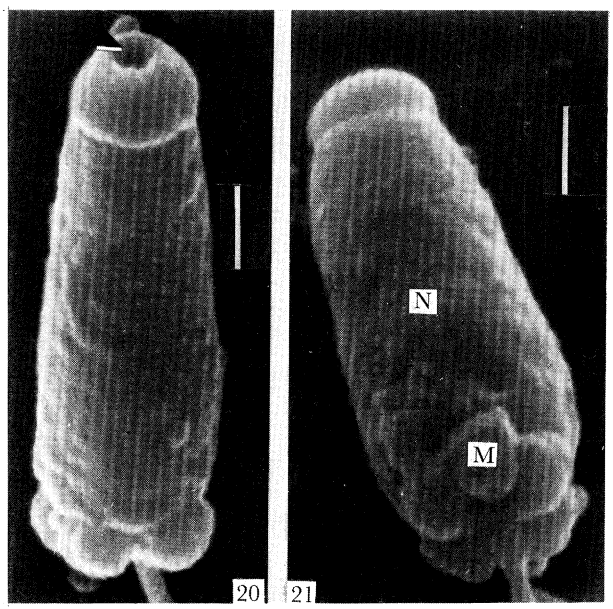

Figures 20 and 21. SEM micrographs of spermatozoa. Note the apical pit of the acrosome (arrowhead in figure 20). Five spherical mitochondria (M) occur at the base of the nucleus (N) (figure 21). Scale bar = 1 μm.

which has been described as an egg-shaped structure filled with fine granular secretion (Buckland-Nicks & Chia 1989), is structurally simpler than that in *A. entalis*.

Furthermore, a conical protrusion of the nucleus extends into the subacrosomal space in *Antalis entalis*. This differs from the occurrence of either a subacrosomal invagination into the nucleus forming the so-called nuclear tunnel in *Musculus discors* (Franzén 1983) or anterior nuclear fossa correlated with the presence of an axial rod in the acrosome reviewed in the Bivalvia by Popham (1979).

Using light microscopy, Franzén (1955) described only minor changes during acrosome formation once the dictyosome came to occupy the apex of the nucleus in *Dentalium entalis*. Ultrastructural studies in *Antalis entalis* provide additional information about the differentiation of the proacrosomal vesical produced by the single Golgi complex. Comparison with other molluscs shows that the number of Golgi complexes occurring during spermiogenesis varies between phylogenetic groups. A single Golgi complex is involved in the production of the proacrosome in examples from the Aplacophora (Buckland-Nicks & Chia 1989), Polyplacophora (Buckland-Nicks *et al.* 1988) and Archaeogastropoda (Azevedo 1981; Buckland-Nicks & Chia 1986; Al-Hajj 1988; Hodgson & Bernard 1988). In bivalves, both single and multiple Golgi complexes occur, for example, a single Golgi complex has been described in *Laternula limicola* (Kubo 1977), *Neotrigonia* (Healy 1989), *Musculus discors*, *Nucula sulcata*, *Dreissena polymorpha* (Franzén 1983), *Donax* (Hodgson *et al.* 1990) and multiple ones in *Mytilus edulis* (Longo & Dornfeld 1967), *Spisula solidissima* (Longo & Anderson 1969) and galeommatoid bivalves (Eckelbarger *et al.* 1990). In mollusc classes with modified spermatozoa, for example, Opisthobranchia (Eckelbarger & Eyster 1981; Kubo & Ishikawa 1981; Medina *et al.* 1985), Pulmonata (Takaichi & Dan 1977) and Cephalopoda (Maxwell 1974, 1975), only multiple Golgi complexes occur. Our studies of spermatogenesis in *A. entalis* provide confirmation of the primitive phylogenetic position of the Scaphopoda.

The migration of the proacrosomal granule from the posterior to the anterior pole of the spermatid in *Antalis entalis* closely parallels the situation observed in other molluscan groups with primitive spermatozoa, for example, the Aplacophora (Buckland-Nicks & Chia 1989), bivalves (Longo & Dornfeld 1967; Longo &

PHILOSOPHICAL TRANSACTIONS OF THE ROYAL SOCIETY B BIOLOGICAL SCIENCES

Anderson 1969; Popham 1979; Healy 1989; Hodgson *et al.* 1990) and archaeogastropods (Azevedo 1981; Hodgson & Bernard 1988; Koike 1985). Once the proacrosomal vesicle becomes apposed to the presumptive apex of the nucleus, its form differentiates from spherical to cup-shaped. In contrast, the Golgi complex migrates to the apex of the nucleus and then forms the proacrosomal granule in molluscan groups with modified spermatozoa, for example, opisthobranchs (Eckelbarger & Eyster 1981; Kubo & Ishikawa 1981), pulmonates (Takaichi & Dan 1977; Rigby 1982) and cephalopods (Maxwell 1974, 1975).

In patellid limpets, the Golgi complex often persists in the late spermatid (Hodgson & Bernard 1988). In *Chaetoderma* sp., the renewed activity of the Golgi body anteriorly even produces an apical horn and an apical tube (Buckland-Nicks & Chia 1989). In *Antalis entalis*, on the contrary, the Golgi complex is lost once the proacrosome has formed at the beginning of the late spermatid stage.

Baccetti & Afzelius (1976) suggest that the increasing complexity of the acrosome is acquired progressively throughout evolution. In recent years many attempts to use acrosome morphology as an indicator for phylogenetic affinities within various molluscan groups have proved valuable and useful (Franzén 1970, 1983; Popham 1979; Kohnert & Storch 1983; Maxwell 1983; Koike 1985; Hodgson & Bernard 1986, 1988; Healy 1988, 1989). Popham (1979) suggests that the organization of the acrosome in bivalves may reflect the systematic or phylogenetic relationship of species within the group. Comparing the mature spermatozoa of *Antalis entalis* with *Dentalium vulgare* shows only minor differences, suggesting that these two species are closely related. Our observations on scaphopod spermiogenesis provide further evidence that the process of acrosome formation may be useful in studies of molluscan systematics and evolution.

Once attachment of the mitochondria to the nuclear envelope and the location of the proacrosome has occurred, then spermatid nuclear elongation proceeds. No manchette or any microtubules occur around the nucleus during this stage. The internal force(s) that change the shape of the spermatid nucleus from spherical to elongate is obscure. In the Aplacophora (Buckland-Nicks & Chia 1989), bivalves (except *Scrobicularia plana* (Sousa *et al.* 1989)) (Longo & Dornfeld 1967; Longo & Anderson 1969; Popham *et al.* 1974; Popham 1979; Maxwell 1983; Healy 1989; Hodgson *et al.* 1990), archaeogastropods (Koike 1986; Al-Hajj 1988; Hodgson & Bernard 1988), all nuclear elongation and chromatin condensation occurs without the presence of a microtubular manchette. The same situation occurs in the scaphopod *A. entalis*. Fawcett *et al.* (1971) postulated that the pattern of chromatin condensation might be an important process in shaping the sperm head. Hodgson & Bernard (1988) also suggested that nuclear elongation might be brought about by forces within the nucleus. Our observations on nuclear development during spermiogenesis in *A. entalis* provide additional support for this hypothesis.

The development of the middle piece resembles that seen in the patellid limpets (Hodgson & Bernard 1988) and bivalves (Longo & Dornfeld 1967; Longo & Anderson 1969; Popham *et al.* 1974; Franzén 1983; Healy 1989; Hodgson *et al.* 1990). Mitochondria are the first organelles to become apposed to the nucleus. These apposed mitochondria then increase their size throughout spermiogenesis. Healy (1989) described numerical differences of mitochondria in the spermatozoa of bivalve taxa, for example, in Pteriomorphia, five or six mitochondria occur in Mytiliidae, four or five in Pterioidea, whereas only four in Ostreoidea, Anomioidea and Acroidea. In scaphopods, however, only five spherical mitochondria occur (Franzén 1955; Dufresne-Dube *et al.* 1983; this study).

In the scaphopods, the distal centriolar satellites are structurally similar to those described in a wide variety of primitive spermatozoa in the models developed by Summers (1970) and Baccetti & Afzelius (1976).

In *Antalis entalis* the axoneme in the flagellum of the spermatozoon consists of a typical '9+2' microtubular structure. Our observations on spermiogenesis of the scaphopod allow us to state that, with the exception of the, as yet uninvestigated Monoplacophora, the '9+2' axonemal organization of the spermatozoon is the only form obtained within the phylum Mollusca.

Glycogen granules accumulate only at the later stages of spermatid development in *Antalis entalis* and are located in the middle piece and close to the acrosome. A perimitochondrial distribution of glycogen has been observed in bivalves (see review, Maxwell 1983), for example, *Nucula sulcata* (Franzén 1983), *Donax* (Hodgson *et al.* 1990), *Divariscintilla* and *Scintilla* sp. (Eckelbarger *et al.* 1990), and the scaphopod *Dentalium vulgare* (Dufresne-Dube *et al.* 1983). Glycogen granules occur in the acrosomal region in scaphopods (Dufresne-Dube *et al.* 1983), bivalves, for example *Donax* (Hodgson *et al.* 1990), Teredinidae (Popham & Dickson 1975), and octopods (Maxwell 1974). There is no storage of glycogen in the tail piece in the so-called 'primitive' type of spermatozoon. We can now confirm a similar glycogen distribution in the spermatozoa of *Antalis entalis* to that described in *D. vulgare*. These glycogen granules are probably sources of energy for motility and metabolism (Anderson & Personne 1970, 1976).

To summarize, this is the first ultrastructural investigation of spermatogenesis in a scaphopod. Its primitive spermatozoon and the process of spermatogenesis demonstrate close parallels with those of bivalves and archaeogastropods with 'primitive' type of spermatozoon. However, its acrosomal organization makes it unique in comparison with that described in any other molluscan group. The present investigation demonstrates that the organization of the microtubular axoneme in scaphopod spermatozoa is exactly comparable to that in other molluscan classes (see reviews, Baccetti & Afzelius 1976; Popham 1979; Maxwell 1983; Koike 1986; Healy 1988).

We thank Professor K. Vickerman for helpful comments on the manuscript and C. P. Palmer, Department of Palaeontology, British Museum (Natural History), for species identification. This work was supported by a Postgraduate Student Scholarship of University of Glasgow and ORS Award to S. T. H.

PHILOSOPHICAL TRANSACTIONS OF THE ROYAL SOCIETY B BIOLOGICAL SCIENCES

REFERENCES

Al-Hajj, H. A. 1988 Ultrastructural analysis of sperm head development in *Nerita polita* (Mollusca: Archaeogastropoda) from the Jordan Gulf of Aqaba (Red Sea). *Int. J. Invert. Rep. Dev.* **13**, 281–295.

Anderson, W. A. & Personne, P. 1970 The localization of glycogen in the spermatozoa of various invertebrate species. *J. Cell Biol.* **44**, 29–51.

Anderson, W. A. & Personne, P. 1976 The molluscan spermatozoon: dynamic aspects of its structure and function. *Am. Zool.* **16**, 293–313.

Azevedo, C. 1981 The fine structure of the spermatozoon of *Patella lusitarica* (Gastropoda: Prosobranchia), with special reference to acrosome formation. *J. submicrosc. Cytol.* **13**, 47–56.

Baccetti, B. & Afzelius, B. A. 1976 The biology of sperm cell. In *Monographs in developmental biology*, vol. 10 (ed. A. Wolsky), pp. 55–56. Basel: S. Karger.

Buckland-Nicks, J. & Chia, F. S. 1986 Formation of the acrosome and basal body during spermiogenesis in a marine snail, *Nerita picea* (Mollusca: Archaeogastropoda). *Gamete Res.* **15**, 13–23.

Buckland-Nicks, J. & Chia, F. S. 1989 Spermiogenesis in *Chaetoderma* sp. (Aplacophora). *J. exp. Zool.* **252**, 308–317.

Buckland-Nicks, J., Koss, R. & Chia, F. S. 1988 The elusive acrosome of chiton sperm. *Int. J. Invert. Rep. Dev.* **13**, 193–198.

Dufresne-Dube, L., Picheral, B. & Guerrier, P. 1983 An ultrastructural analysis of *Dentalium vulgare* (Mollusca, Scaphopoda) gametes. *J. Ultrastruct. Res.* **83**, 242–257.

Eckelbarger, K. J. & Eyster, L. S. 1981 An ultrastructural study of spermatogenesis in the Nudibranch mollusc *Spurilla neapolitana*. *J. Morph.* **170**, 283–299.

Eckelbarger, K. J., Bieler, R. & Mikkelsen, P. M. 1990 Ultrastructure of sperm development and mature sperm morphology in three species of commensal bivalves (Mollusca: Galeommatoidea). *J. Morph.* **205**, 63–75.

Fawcett, D. W., Anderson, W. A. & Phillips, D. M. 1971 Morphogenetic factors influencing the shape of the sperm head. *Devl Biol.* **26**, 220–251.

Franzén, A. 1955 Comparative morphological investigations into the spermiogenesis among mollusca. *Zool. Bidr. Upps.* **30**, 399–456.

Franzén, A. 1970 Phylogenetic aspects of the morphology of spermatozoa and spermiogenesis. In *Comparative spermatology* (ed. B. Baccetti), pp. 29–46. New York: Academic Press.

Franzén, A. 1983 Ultrastructural studies of spermatozoa in three bivalve species with notes on evolution of elongated sperm nucleus in primitive spermatozoa. *Gamete Res.* **7**, 199–214.

Galtsoff, P. S. & Philpott, D. E. 1960 Ultrastructure of the spermatozoon of the oyster, *Crassostrea virginica*. *J. Ultrastruc. Res.* **3**, 241–253.

Healy, J. M. 1988 Sperm morphology and its systematic importance in the Gastropoda. *Malac. Rev.* (Suppl.) **4**, 251–266.

Healy, J. M. 1989 Spermiogenesis and spermatozoa in the relict bivalve genus *Neotrigonia*: relevance to trigonioid relationships particularly Unionoidea. *Mar. Biol.* **103**, 75–85.

Hinsch, G. W. & Clark, W. H. 1973 Comparative fine structure of cnidaria spermatozoa. *Bio. Reprod.* **8**, 62–73.

Hodgson, A. N. & Bernard, R. T. F. 1986 Observation on the ultrastructure of the spermatozoon of two mytilids from the south-west coast of England. *J. Mar. Biol. Ass. U.K.* **66**, 385–390.

Hodgson, A. N. & Bernard, R. T. F. 1988 A comparison of the structure of the spermatozoa and spermatogenesis of 16 species of patellid limpet (Mollusca: Gastropoda: Archaeogastropoda). *J. Morph.* **195**, 205–223.

Hodgson, A. N., Baxter, J. M., Sturrock, M. G. & Bernard, R. T. F. 1988 Comparative spermatology of 11 species of Polyplacophora (Mollusca) from the suborders Lepidopleurina, Chitonina and Acanthochitonina. *Proc. R. Soc. Lond.* B **235**, 161–177.

Hodgson, A. N., Bernard, R. T. F. & Van der Horst, G. 1990 Comparative spermatology of three species of *Donax* (Bivalvia) from South Africa. *J. mollusc. Stud.* **56**, 257–265.

Kohnert, R. & Storch, V. 1983 Ultrastrukturelle untersuchungen zur morphologie und genese der spermien von Archaegastropoda. *Helgoländer wiss. Meeresunters.* **36**, 77–84.

Koike, K. 1985 Comparative ultrastructural studies on the spermatozoa of the Prosobranchia (Mollusca: Gastropoda). *Sci. Rep. Fac. Educ. Gunma. Univ.* **34**, 33–153.

Kubo, M. 1977 The formation of a temporary-acrosome in the spermatozoa of *Laternula limicola* (Bivalvia, Mollusca). *J. Ultrastruct. Res.* **61**, 140–148.

Kubo, M. & Ishikawa, M. 1981 Organisation of the acrosome and helical structure in sperm of the Aplysiid, *Aplysia kurodai* (Opisthobranchia). *Differentiation* **20**, 131–140.

Longo, F. J. & Anderson, E. 1969 Spermiogenesis in the surf clam *Spisula solidissima* with special reference to the formation of the acrosomal vesicle. *J. Ultrastruct. Res.* **27**, 435–443.

Longo, F. J. & Dornfeld, E. G. 1967 The fine structure of spermatid differentiation in the mussel, *Mytilus edulis*. *J. Ultrastruct. Res.* **20**, 462–480.

Maxwell, W. L. 1974 Spermiogenesis of *Eledone cirrhosa* Lamark (Cephalopoda, Octopoda). *Proc. R. Soc. Lond.* B **186**, 181–190.

Maxwell, W. L. 1975 Spermiogenesis of *Eusepia officinalis* (L.), *Loligo forbesi* (Steenstrup) and *Alloteuthis subulata* (L.) (Cephalopoda, Decapoda). *Proc. R. Soc. Lond.* B **191**, 527–535.

Maxwell, W. L. 1983 Mollusca. In *Reproductive biology of invertebrates*, vol. II (*Spermatogenesis and sperm function*) (ed. K. G. Adiyodi & R. G. Adiyodi), pp. 275–319. John Wiley and Sons.

Medina, A., Moreno, J. & López-Campos, J. L. 1985 Acrosome evolution in *Hypselodoris tricolor* (Gastropoda: Nudibranchia). *J. submicrosc. Cytol.* **17**, 404–411.

Niijima, L. & Dan, J. 1965 The acrosome reaction in *Mytilus edulis*. I: fine structure of the intact acrosome. *J. Cell Biol.* **25**, 243–248.

Popham, J. D. 1979 Comparative spermatozoon morphology and bivalve phylogeny. *Malac. Rev.* **12**, 1–20.

Popham, J. D. & Dickson, M. R. 1975 Location of glycogen in spermatids and spermatozoa of the shipworm, *Bankia australis* (Teredinidae, Bivalvia, Mollisca). *Cell Tiss. Res.* **164**, 519–524.

Popham, J. D., Dickson, M. R. & Goddard, C. K. 1974 Ultrastructural study of the mature gametes of two species of *Bankia* (Mollusca: Teredinidae). *Aust. J. Zool.* **22**, 1–12.

Retzius, G. 1905 Zur kenntnis der spermien der Evertebraten. II. *Biol. Untersuch.* (NF) **12** (9), 101–102. Taf. XI–XIX.

Rigby, J. E. 1982 The fine structure of differentiating spermatozoa and Sertoli cells in the gonad of the pond snail, *Lymnaea stagnalis*. *J. mollusc. Stud.* **48**, 111–123.

Russell-Pinto, F., Azevedo, C. & Oliveira, E. 1984 Comparative ultrastructural studies of spermiogenesis and spermatozoa in some species of Polyplacophora (Mollusca). *Int. J. Invert. Rep. Dev.* **7**, 267–277.

Sakker, E. R. 1984 Sperm morphology, spermatogenesis

and spermiogenesis of three species of chitons (Mollusca, Polyplacophora). *Zoomorphology* **104**, 111–121.

Sousa, M., Corral, L. & Azevedo, C. 1989 Ultrastructural and cytochemical study of spermatogenesis in *Scrobicularia plana* (Mollusca, Bivalvia). *Gamete Res.* **24**, 393–401.

Summers, R. G. 1970 A new model for the structure of the centriolar satellite complex in spermatozoa. *J. Morph.* **137**, 229–242.

Takaichi, S. & Dan, J. C. 1977 Spermiogenesis in the pulmonate snail, *Euhadra hickonis*. I. Acrosome formation. *Develop. Growth Differ.* **19**, 1–14.

Thiéry, J. 1967 Mise en évidence des polysaccharides sur coupes fines en microscopie électronique. *J. Microsc.* **7**, 987–1019.

Vye, M. V. & Fischman, D. A. 1971 A comparative study of three methods for the ultrastructural demonstration of glycogen in thin sections. *J. Cell Sci.* **9**, 724–749.

Received 1 February 1991; accepted 8 April 1991

PHILOSOPHICAL TRANSACTIONS OF THE ROYAL SOCIETY B BIOLOGICAL SCIENCES

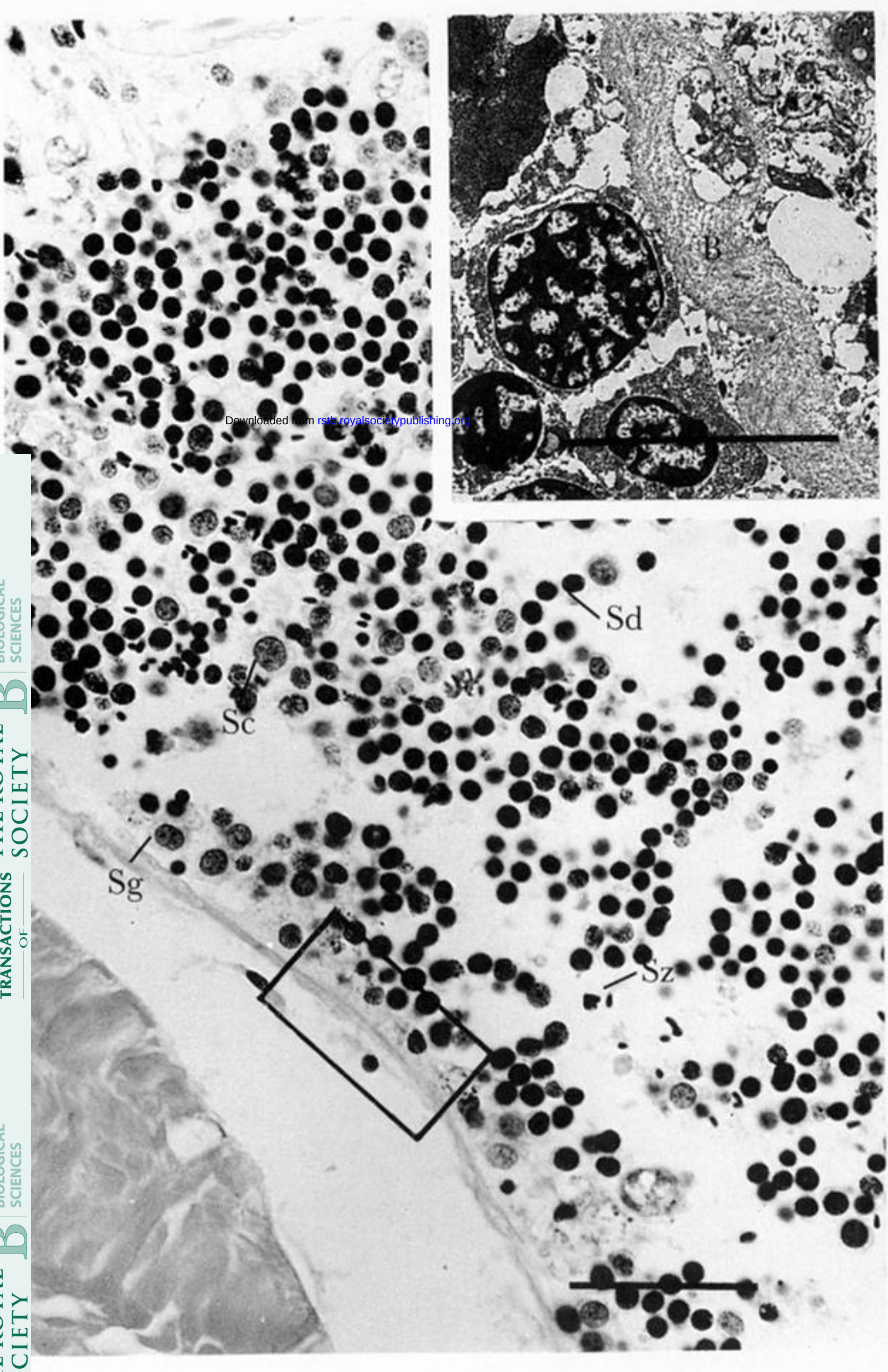

PHILOSOPHICAL TRANSACTIONS OF THE ROYAL SOCIETY B BIOLOGICAL SCIENCES

gure 1. Light micrograph through part of the testis, owing part of a testicular follicle and developing germ ls (spermatogonium, Sg; spermatocyte, Sc; spermatid, and spermatozoon, Sz). The rectangular area is enlarged show the fibrillar basement membrane (B, inset; scale r = 10 μm). Scale bar = 50 μm.

igure 2. A spermatogonium with a prominent nucleolus Ne), and many small mitochondria (M). Scale bar = 1 μm.

PHILOSOPHICAL TRANSACTIONS OF THE ROYAL SOCIETY B BIOLOGICAL SCIENCES

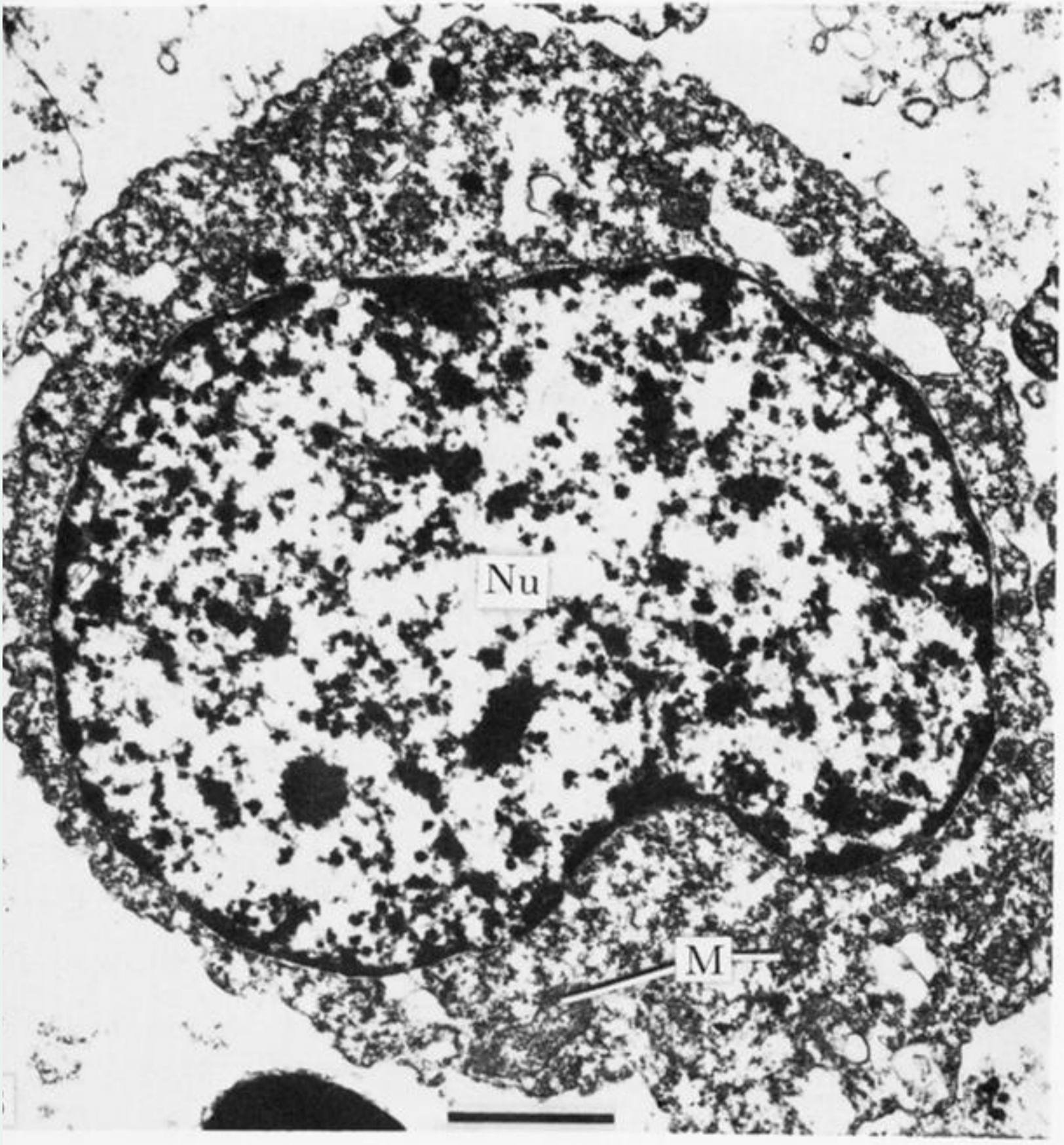

igure 3. A secondary spermatocyte with diffuse hetero-
romatin in the nucleus (Nu). The mitochondria (M) are
nall. Scale bar = 1 μm.

PHILOSOPHICAL TRANSACTIONS OF THE ROYAL SOCIETY B BIOLOGICAL SCIENCES

gure 4. Two nuclei (Nu) of early spermatids occur within a single mass of cytoplasm. Scale bar = 1 μm.

PHILOSOPHICAL TRANSACTIONS OF THE ROYAL SOCIETY B BIOLOGICAL SCIENCES

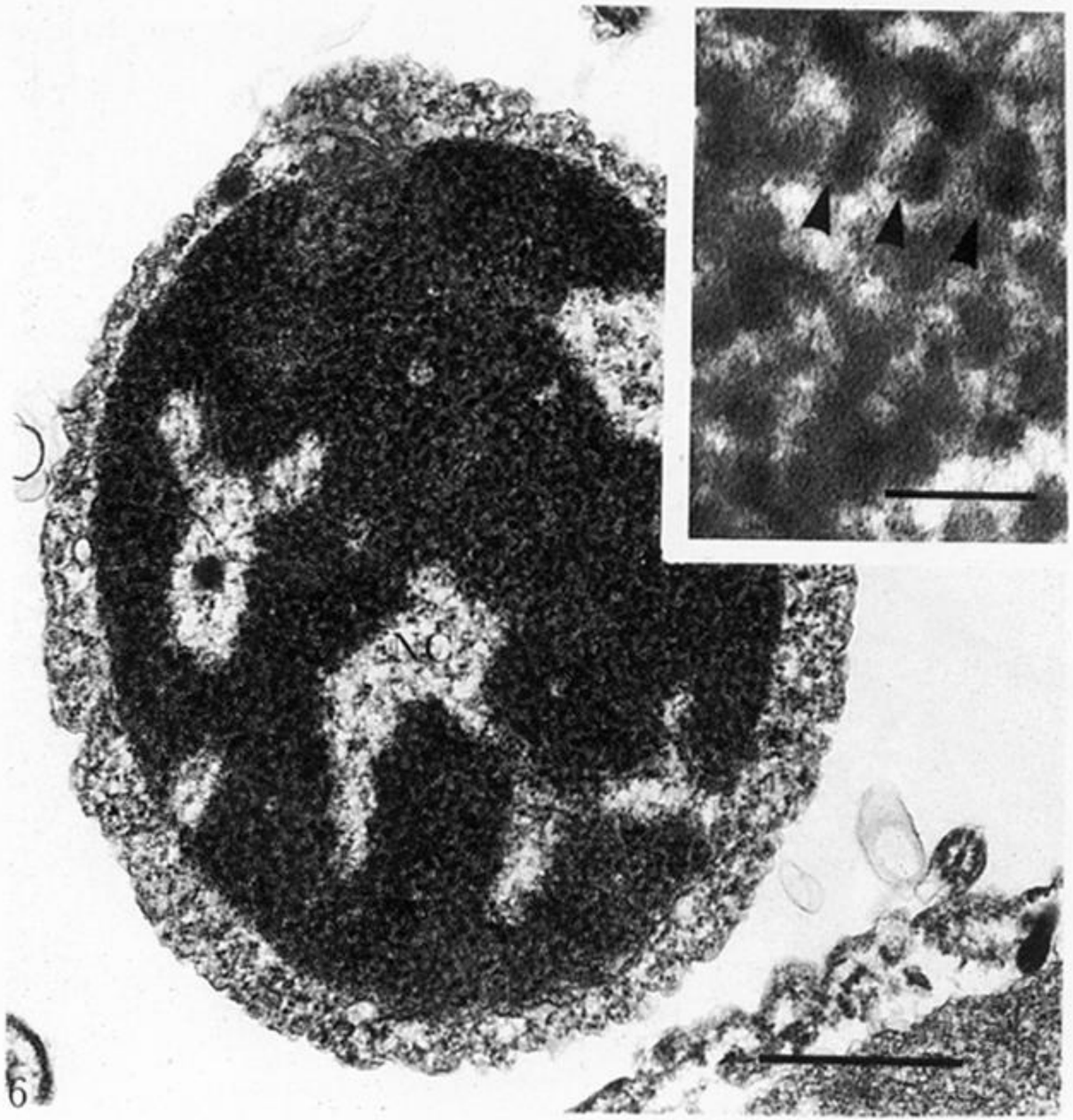

Figures 5 and 6. Sections through early (figure 5) and late (figure 6) spermatids, showing the granular heterochromatin (arrowheads in figure 5 and inset) aggregating into an almost homogeneous state (figure 6 and inset). Because of uneven chromatin condensation, small nuclear cavities (NC) remain (figure 6). Scale bars = 1 μm (0.1 μm for insets).

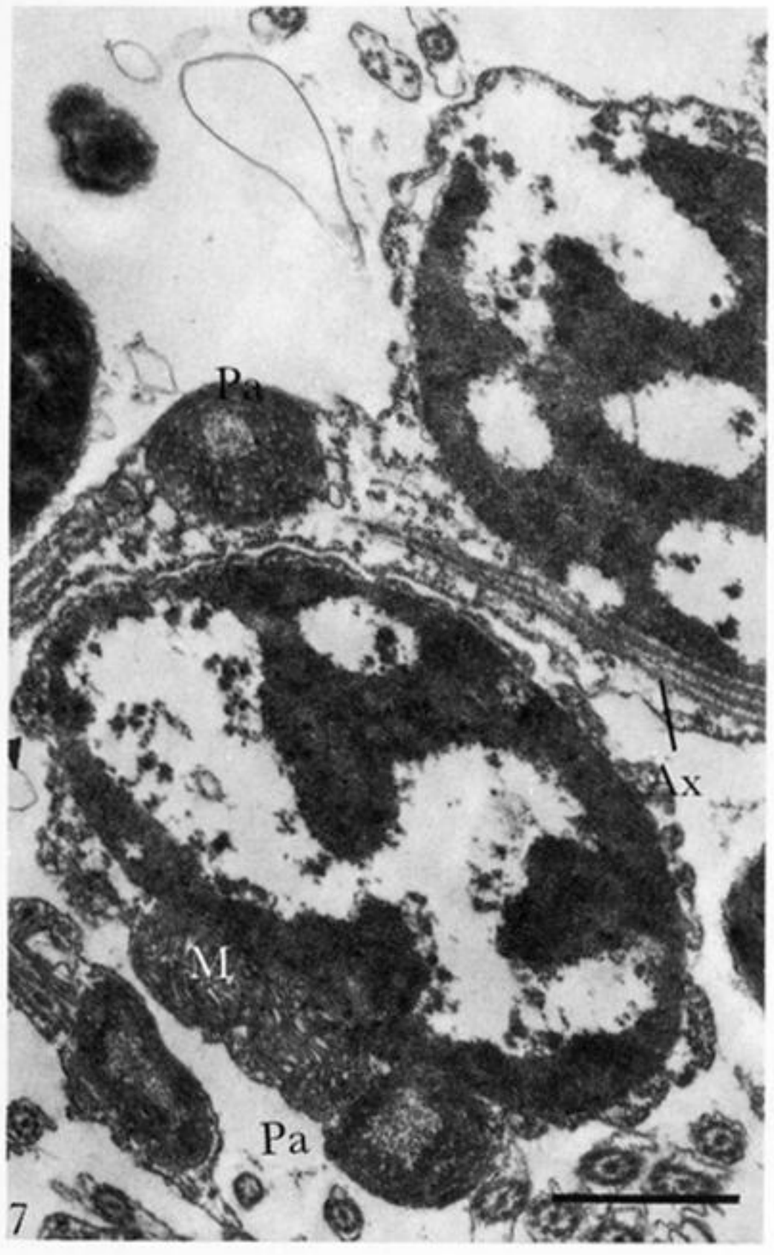

7

8

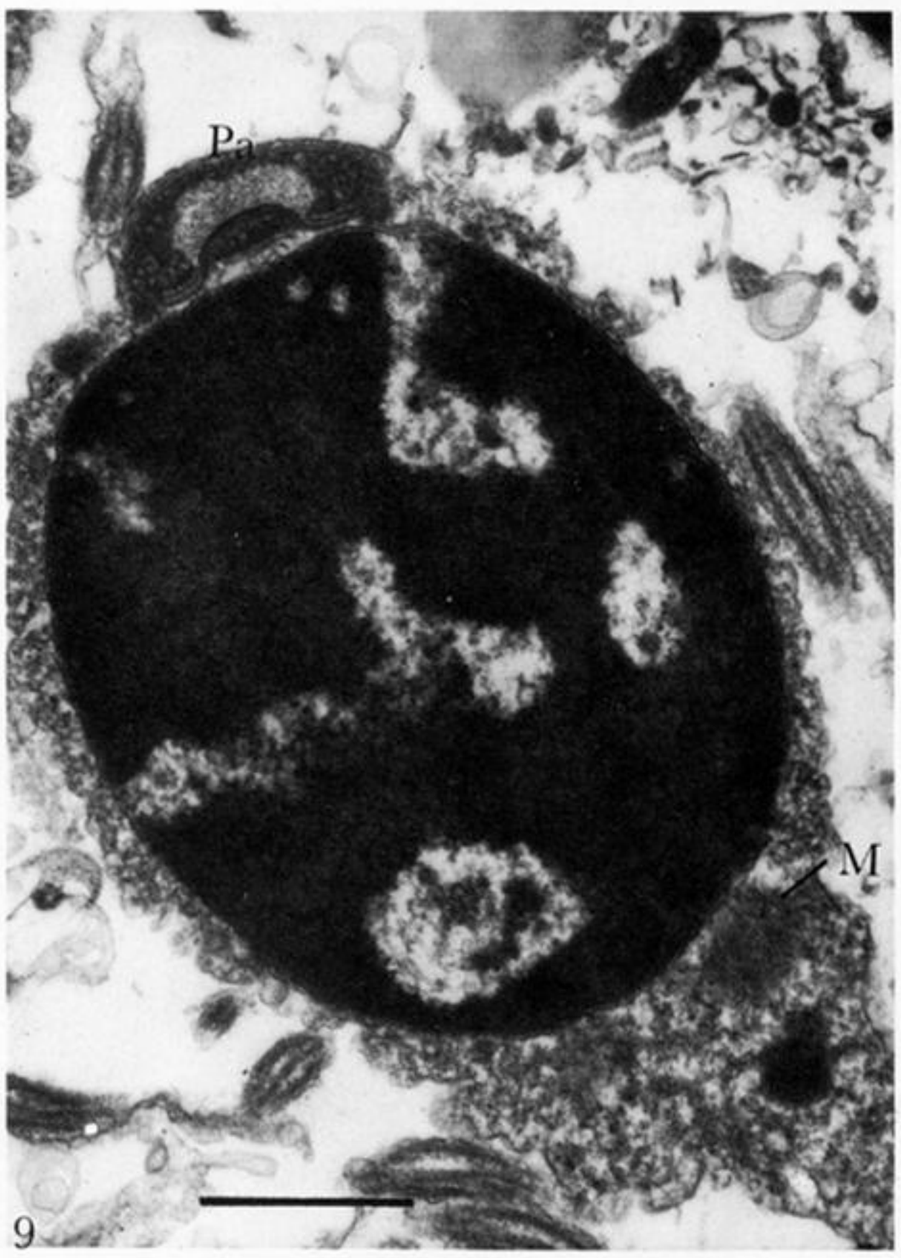

9

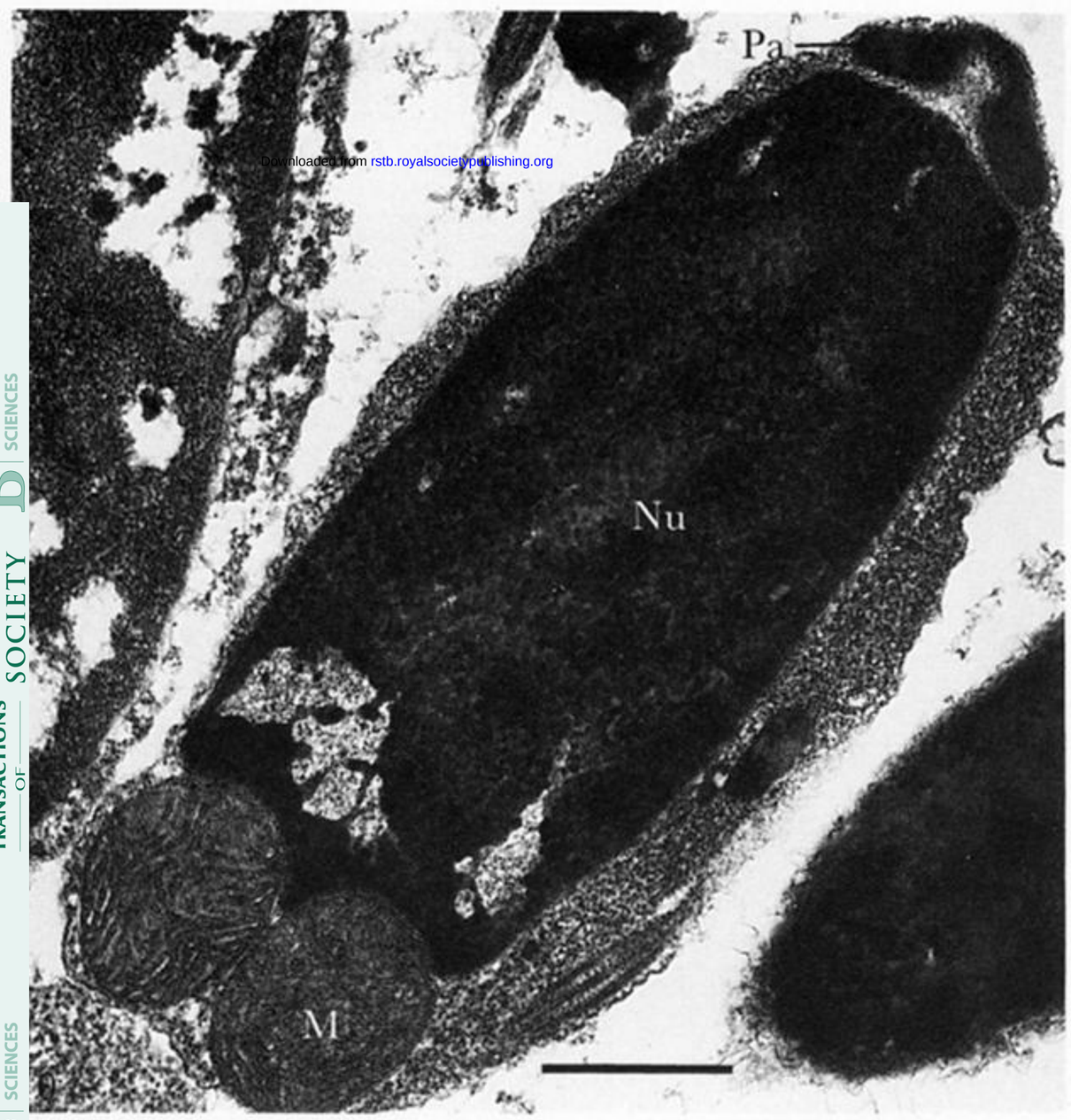

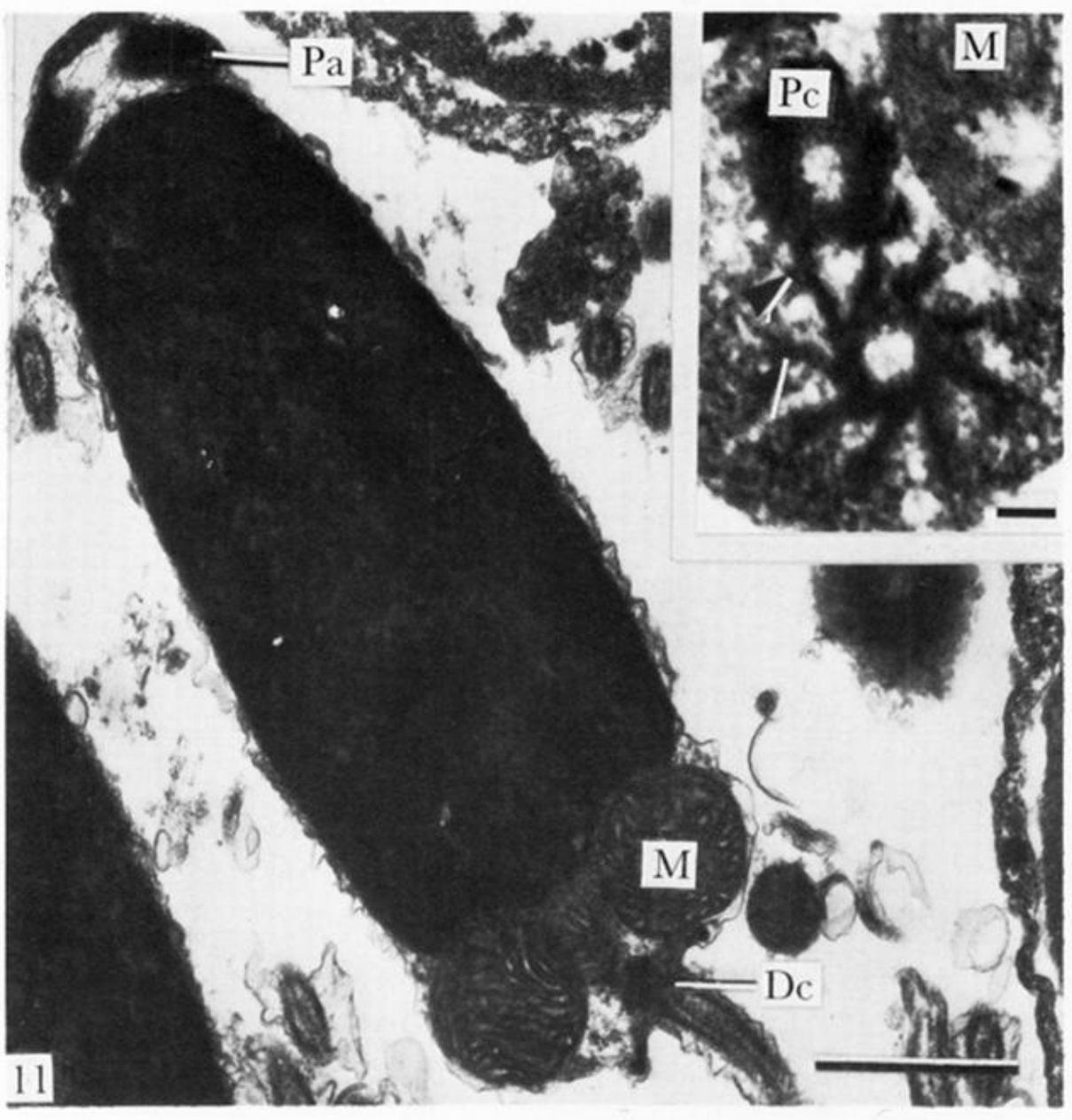

11

Figures 7–11. Ultrathin sections of developing early spermatids (figures 7 and 8) and late spermatids (figures 9–11). Nuclear morphogenesis results in a change from an oval shape (figure 7) to an elongate one (figures 10 and 11). The proacrosomal granule (Pa) is in close relation to mitochondria (M), axoneme (Ax) and plasmalemma in the early spermatid (figures 7 and 8) where the granular heterochromatin is still diffuse. Once the mitochondria are attached to the base of the nuclear envelope and increase in size (figure 8), the proacrosome starts to move towards the presumptive anterior pole of the spermatid. Figures 9–11 show the further condensation and elongation of the nucleus of the late spermatid and the loss of excess cytoplasm. The proximal centriole (Pc) and distal centriolar satellite (Dc) with nine radial arms (arrowheads) are fully established at this developmental stage (figure 11 inset). Scale bars = 1 μm (0.1 μm for inset).

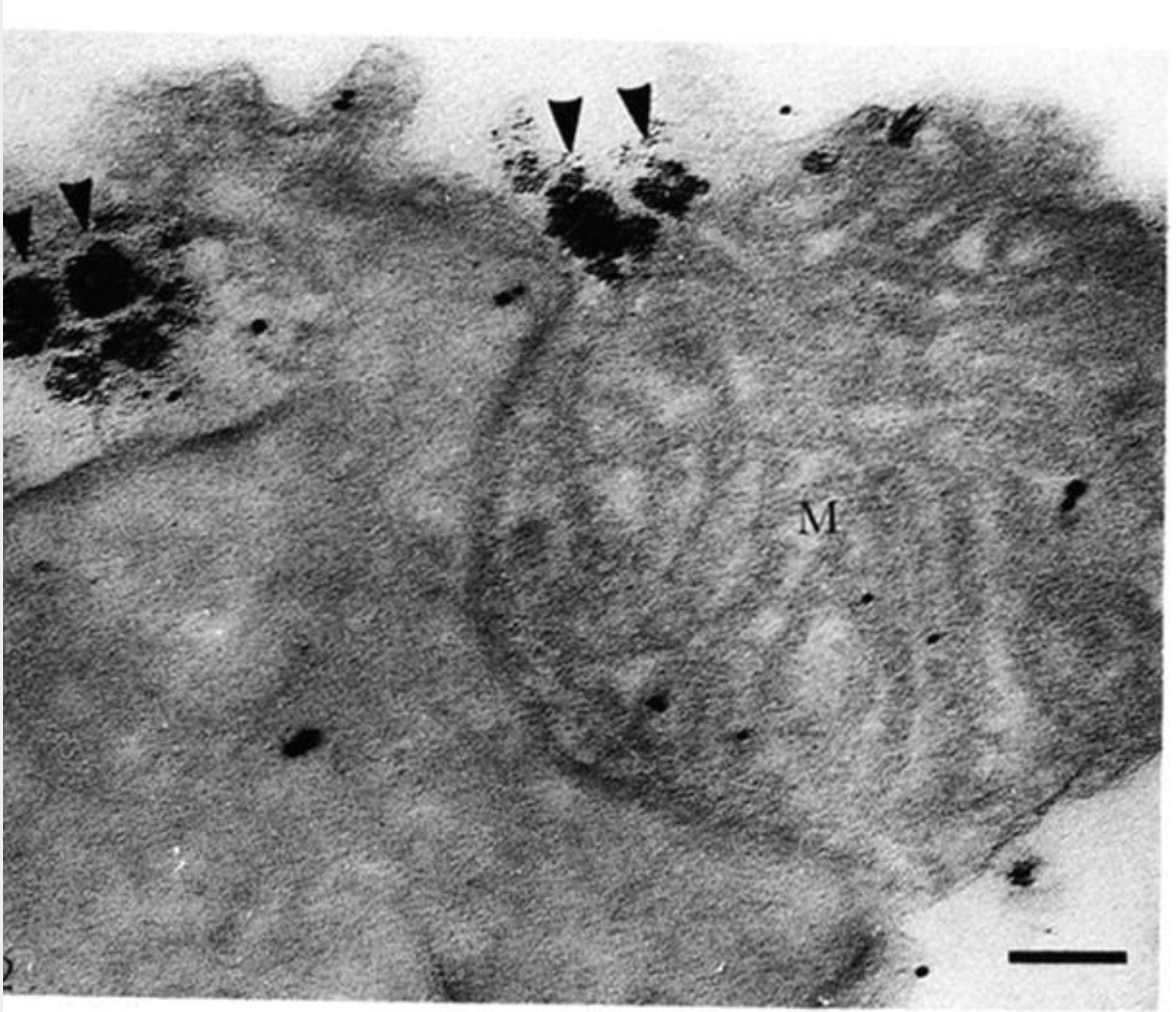

gure 12. PA-TSC-SP treated late spermatid. Dark glycogen anules (arrowheads) occur around mitochondria (M). ale bar = 0.1 μm.

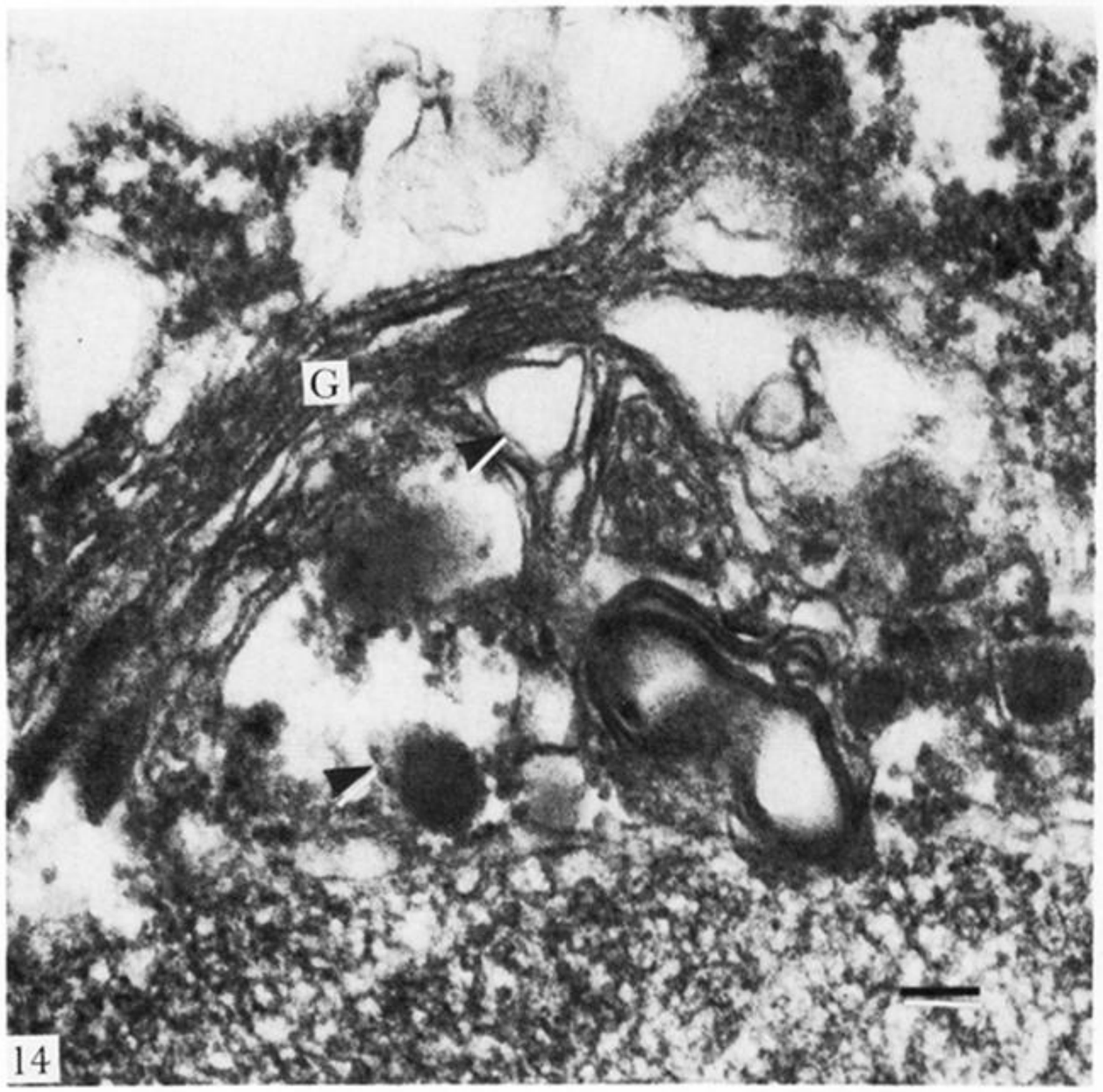

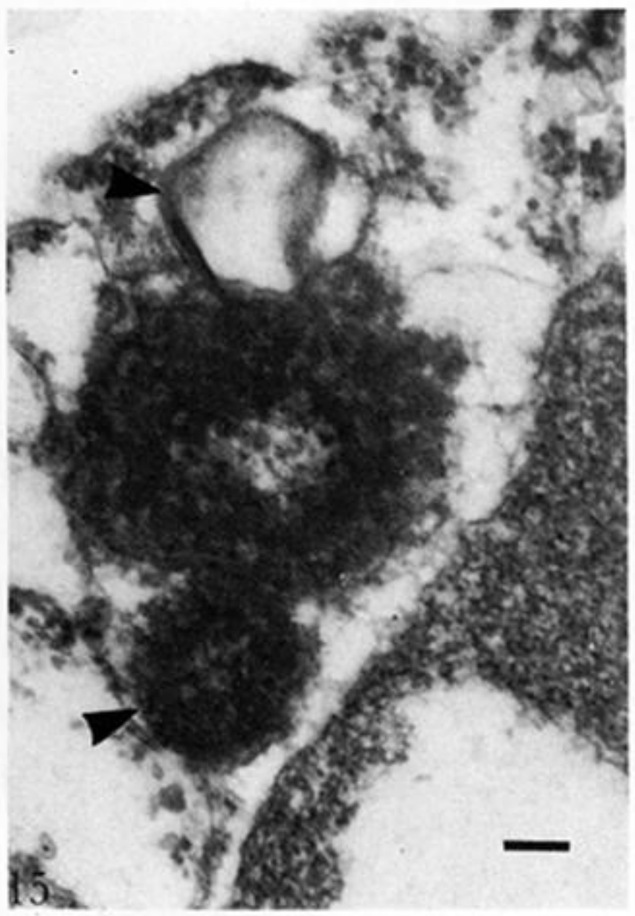

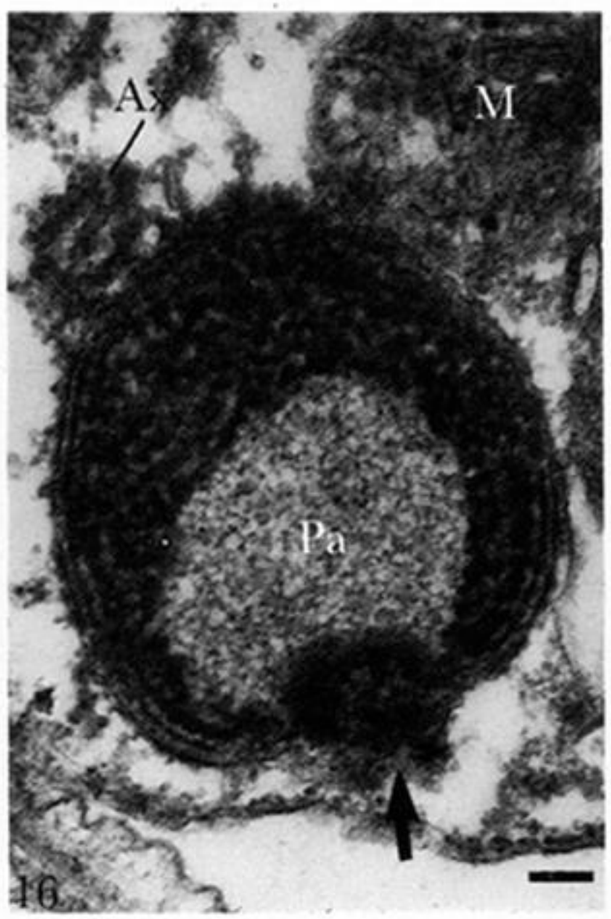

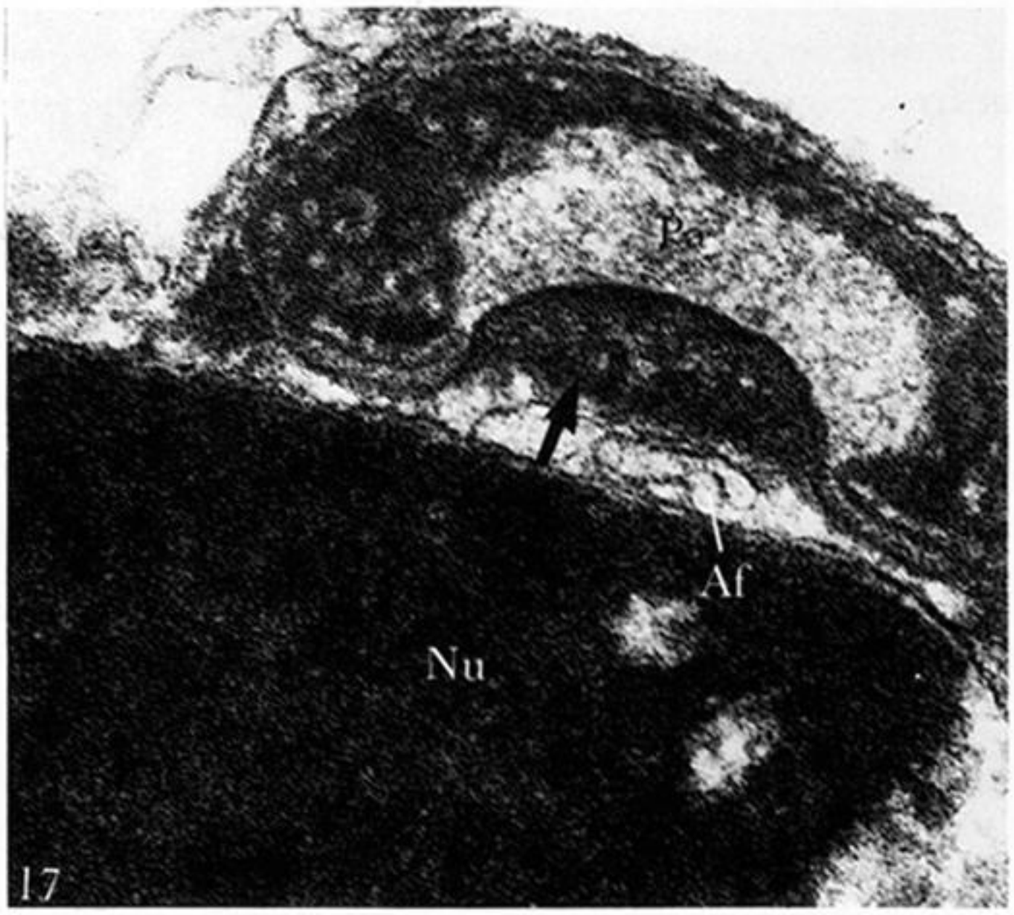

Figures 13–17. For description see opposite.

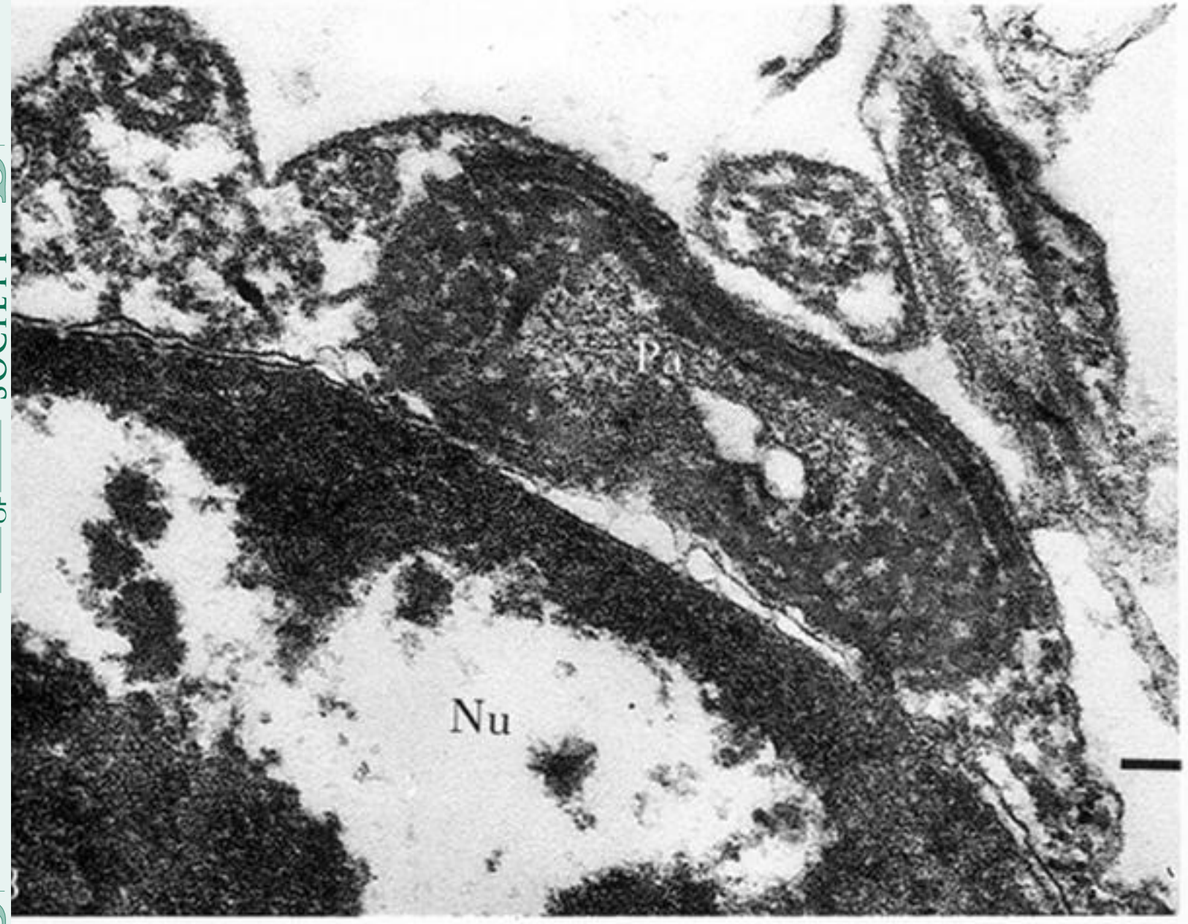

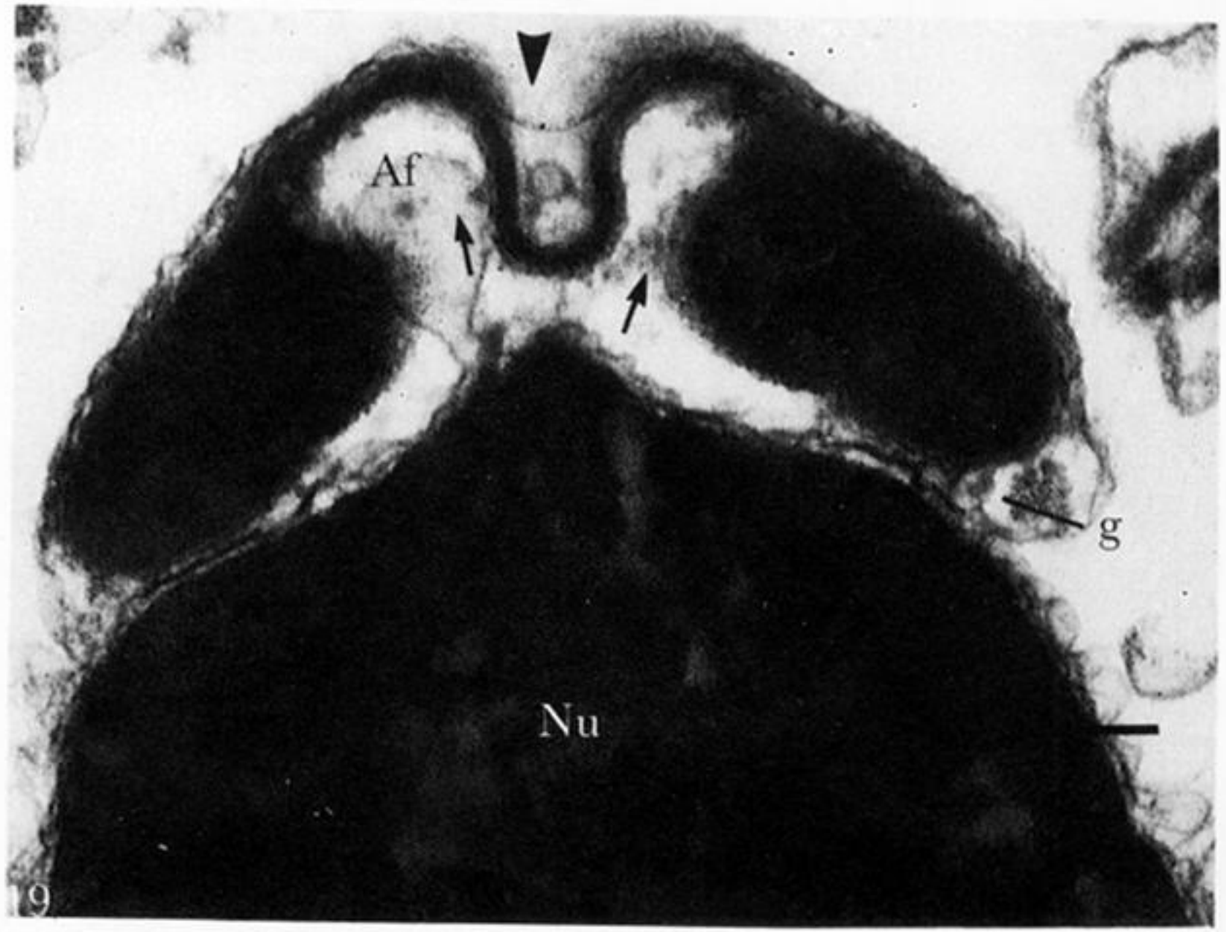

Figures 13–19. Stages of acrosome development from early spermatid (figures 13–16) to late spermatid (figures 17–19). In the early spermatid, the Golgi complex (G), mitochondria (M) and axoneme (Ax) are closely associated (figure 13). The distal centriole (Dc) at this stage lacks a supporting satellite body. Electron dense granules and lucent vesicles (arrowheads) fuse to form a proacrosomal granule (Pa) (figures 14–16). During the course of migration from the posterior to anterior pole of the spermatid, the electron-dense zone (arrows in figures 16 and 17) becomes closely related to the nucleus and gradually disperse into a layer of dense fibrous material (arrows in figure 19). The proacrosome undergoes significant morphogenesis, converting a spherical (figure 16) to a cup-shape with an inverted central pit (arrowhead) into the underlying acrosomal fossa (Af) (figures 17 and 19). Note a glycogen granule (g) close to the acrosome. Scale bar = 0.1 μm for all parts.

PHILOSOPHICAL TRANSACTIONS OF THE ROYAL SOCIETY B BIOLOGICAL SCIENCES

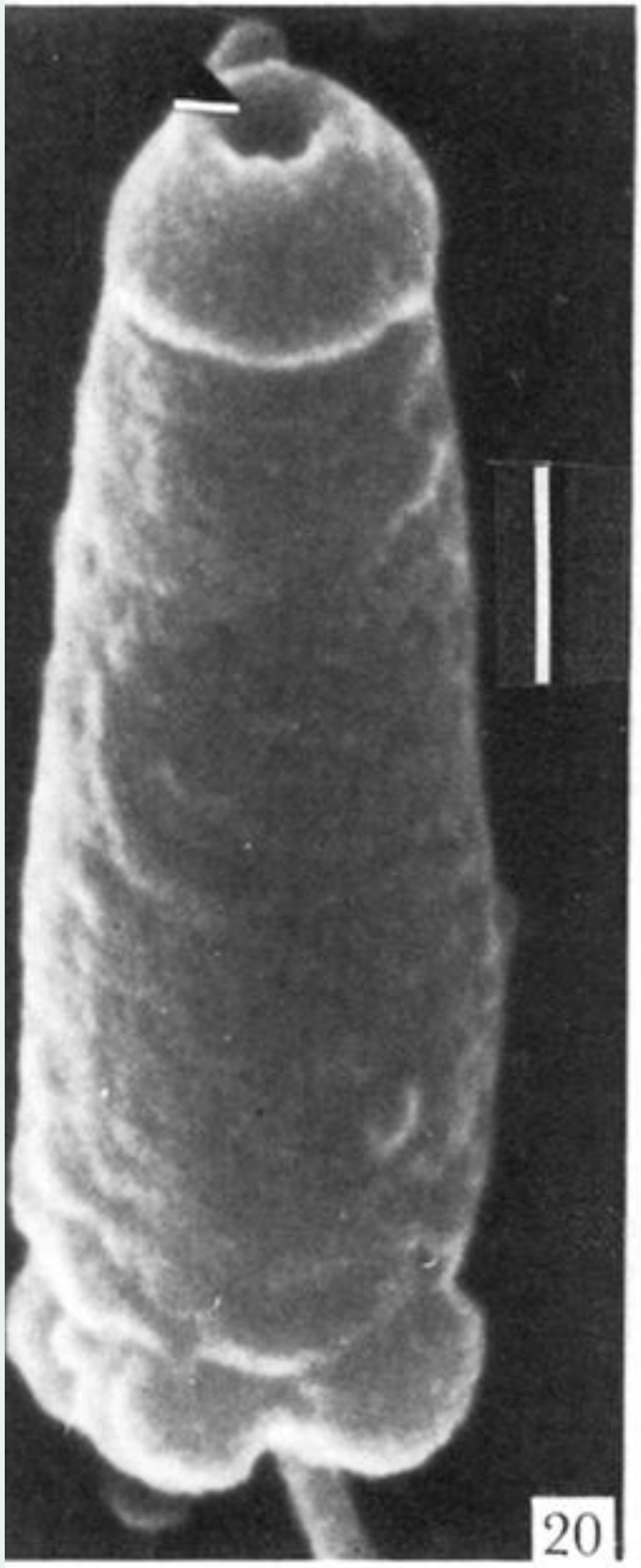

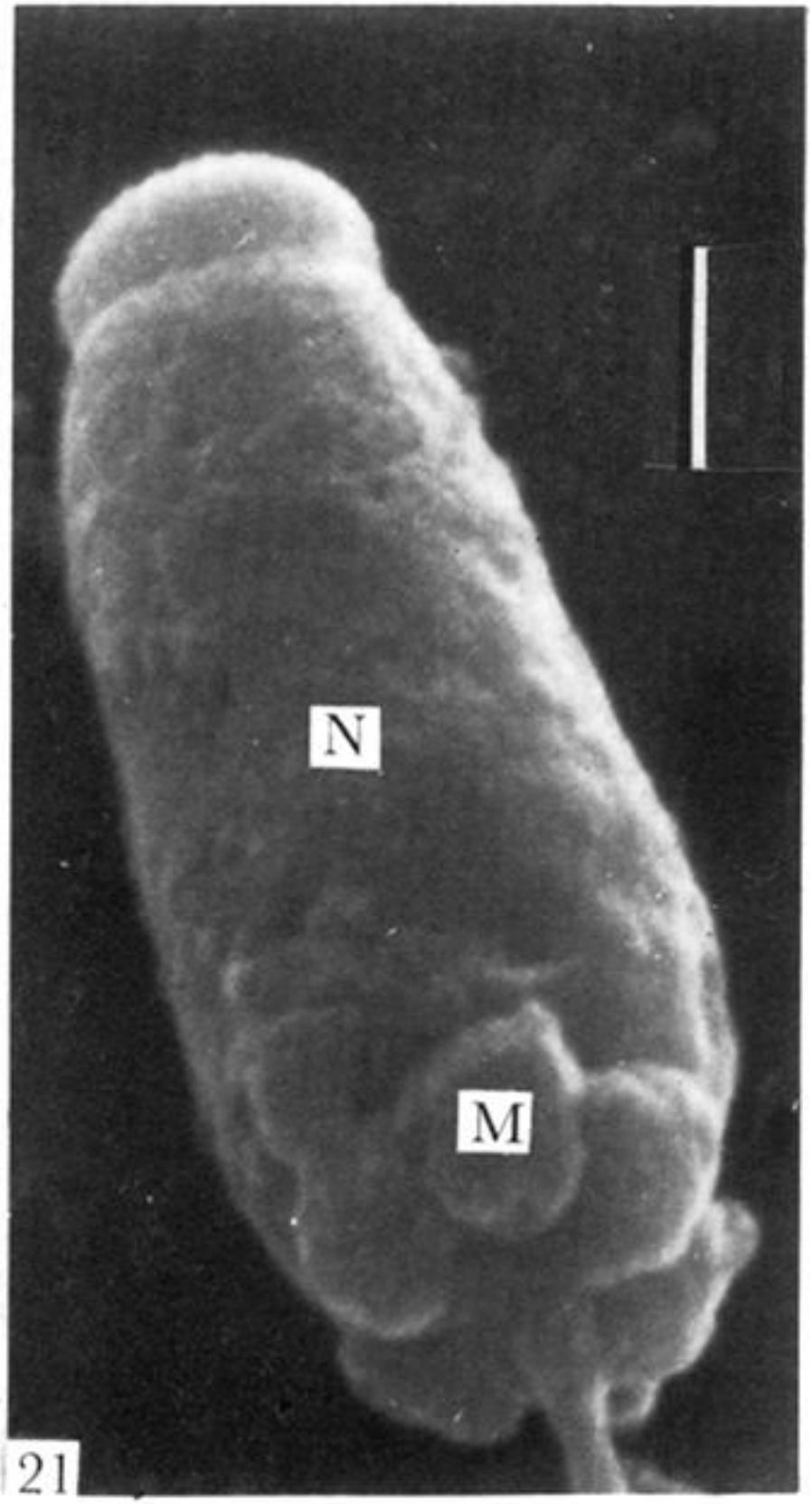

gures 20 and 21. SEM micrographs of spermatozoa. Note the ical pit of the acrosome (arrowhead in figure 20). Five herical mitochondria (M) occur at the base of the nucleus N) (figure 21). Scale bar = 1 μm.

PHILOSOPHICAL TRANSACTIONS OF THE ROYAL SOCIETY B BIOLOGICAL SCIENCES